2019•2020

Faculteit Industriële ingenieurswetenschappen

master in de industriële wetenschappen: energie

Masterthesis

Characterisation of electrode size regarding upscaling in microbial fuel cells for optimising bio-electricity harvesting

PROMOTOR :

Prof. dr. ir. Michael DAENEN

PROMOTOR :

Prof. dr. Jean MANCA

BEGELEIDER :

dra. Thessa VAN LIMBERGEN

drs. Robin BONNE

Hendrik Emonds

Scriptie ingediend tot het behalen van de graad van master in de industriële wetenschappen: energie, afstudeerrichting elektrotechniek

Gezamenlijke opleiding UHasselt en KU Leuven

2019 • 2020

Faculteit Industriële ingenieurswetenschappen

master in de industriële wetenschappen: energie

Masterthesis

Characterisation of electrode size regarding upscaling in microbial fuel cells for optimising bio-electricity harvesting

PROMOTOR :

Prof. dr. ir. Michael DAENEN

PROMOTOR :

Prof. dr. Jean MANCA

BEGELEIDER :

dra. Thessa VAN LIMBERGEN

drs. Robin BONNE

Hendrik Emonds

Scriptie ingediend tot het behalen van de graad van master in de industriële wetenschappen: energie, afstudeerrichting elektrotechniek

UHASSELT

KU LEUVEN

Deze masterproef werd geschreven tijdens de COVID-19 crisis in 2020. Deze wereldwijde gezondheidscrisis heeft mogelijk een impact gehad op de opdracht, de onderzoekshandelingen en de onderzoeksresultaten.

Woord vooraf

Wanneer ik terugkijk op de afgelegde weg, ben ik zeer blij met het team waarmee ik mocht samenwerken en het onderwerp dat ik kon onderzoeken. Dit ging niet steeds vanzelfsprekend omwille van de COVID-19 pandemie. Toch kon er steeds een oplossing worden gezocht en er stonden velen voor mij klaar die een dankbetuiging verdienen.

Allereerst wil ik de mensen van X-LAB bedanken: Prof. dr. Manca voor zijn enthousiasme en input om mijn thesis in de juiste richting te sturen. Drs. Robin Bonné, dra. Thessa Van Limbergen en dr. Rob Cornelissen mogen zeker niet ontbreken. Zij stonden 24/24 voor mij klaar en probeerden mij in alle richtingen en omwille van COVID-19 te helpen indien nodig. Ze hielpen mij met input en uitleg over de experimenten (die helaas niet konden doorgaan). Het was ook zeer handig om die ervaren begeleiding te hebben zodat ik in dit brede onderwerp toch nog het bos door de bomen kon vinden. Natuurlijk wil ik Prof. dr. ir. Michaël Daenen niet vergeten voor zijn input in het DOE en het in algemeen goede banen leiden van de masterproef. Prof. dr. Ter Heijne wil ik bedanken om haar data van een van haar onderzoeken aan mij ter beschikking te stellen om analyse en fits op uit te voeren. De mensen van de G6 sluiten dat lijstje mooi af met hun morele steun, de gezellige babbel en de taart die de mindere dagen toch beter maakten. Aan iedereen een dikke merci!

Daarnaast wil ik mijn familie bedanken voor hun steun: Lotte voor de babbel, de motivatie en om in mij te blijven geloven. Mijn ouders, broers en schoonouders omdat ik bij hun ook steeds terecht kan en ze de werklast in het huishouden helpen verlichten. Tot slot wil ik, bij het schrijven van dit laatste eindwerk, mijn ouders bedanken voor het bekostigen van mijn studies.

Aan iedereen, bedankt!

Hendrik

Contents

List of Tables

List of Figures

List of abbreviations

COD	Chemical Oxygen Demand
CPE	Constant Phase Element
CW	Constructed Wetlands
DOE	Design of experiments
EA	Electron Acceptors
ECM	Equivalent Circuit Model
MET	Microbial Electrochemical Technology
V_{OC}	Open Circuit Voltage
PEM	Proton Exchange Membrane
(P/S)MFC	(Plant/Sediment) Microbial Fuel Cell

Abstract

Microbial Fuel Cells (MFCs) are bio-electrical systems in which exoelectrogenic bacteria oxidise compounds to produce electricity. The investigation of the correlation between geometrical configurations of MFCs to enhance electrical power output has been an ongoing research. The goal in this research at the X-LAB group of Hasselt University was to obtain design rules for appropriate upscale engineering. A matrix of MFCs with variable parameters (e.g; radius/volume) was made and fits were used to acquire a systematic electrical characterisation regarding the targeted design and output relations.

Electrical impedance spectroscopy was used for characterisation with polarization curves, Nyquist- and Bode plots can give more insight into the impedances of MFCs.

Literature proposed in this work that materials and configurations influence the system's electrical power density. The design of experiments contains a proposed next generation test matrix to measure the influence of electrode radius/volume on the electrical power output. Fits in ZView validate an existing equivalent circuit model for the anode chamber. The efficiency of different MFCs cannot be compared because there is no golden standard to measure energy efficiency or to compare power densities. For this reason further research is required. Experiments on a H-cell and sediment MFC following the written experiment protocol and data analysis methods in ZView could give more conclusive answers in the future.

Abstract in het Nederlands

Microbial Fuel Cells (MFCs) zijn bio-elektrische systemen waarin elektrogene bacteriën organische stoffen oxideren en hierbij elektriciteit produceren. Hedendaags onderzoek probeert een correlatie te vinden tussen de geometrische configuratie van MFCs en het corresponderende elektrische vermogen. Het doel in dit onderzoek in de X-LAB groep van Universiteit Hasselt was het verkrijgen van ontwerpregels voor opschaling. Een MFC testmatrix met variërende parameters (vb. straal/volume) werd ontworpen. Fits werden gebruikt om een gewenste elektrische karakterisatie van een ontworpen design te bekomen.

Elektrische impedantiespectroscopie werd gebruikt voor de karakterisatie met polarisatiecurves, Nyquist-en Bodeplots om meer inzicht te verkrijgen in de impedanties van MFCs.

Literatuur toont aan dat materialen en configuraties het elektrische vermogen van het systeem beïnvloeden. Het design of experiments bevat een voorstel voor een nieuwe generatie testmatrix om de invloed van de elektrodegrootte op het elektrische vermogen te bepalen. Fits in ZView bevestigen een bestaand elektrisch equivalent schema voor de anodekamer. De efficiëntie van verschillende MFCs kan niet met elkaar worden vergeleken omdat er geen gouden standaard is om deze efficiëntie te bepalen of te vergelijken met vermogensdichtheid. Om die reden is er verder onderzoek nodig. Experimenten op een H-cell en sediment MFC volgens de beschreven protocols en data-analyse methodes in ZView kunnen meer sluitende antwoorden geven in de toekomst.

Chapter 1

Introduction

1.1 State-of-the-art

Microbial Fuel Cells (MFCs) are bio-electrical systems in which microorganisms oxidise compounds to produce electricity. In the early twentieth century, M.C. Potter published a study which suggested that certain bacteria species like *Saccharomyces Cerevisiæ* were able to generate electricity when consuming organic compounds [1]. Little credit was given to the study and it took almost two decades until B. Cohen could produce 35 volts with a current of 2 miliamps, using a series of half-cells and bacteria species [2]. Afterwards, some issues due to the unstable nature of hydrogen production by the bacteria were difficult to solve. Therefore only half a century later, Suzuki et. al [3] were able to solve these problems, which led to the first full functioning system called a microbial fuel cell. A basic MFC contains two electrodes (anode and cathode), an electromotive force driven by bacteria, a conductive circuit and a medium or proton barrier between the electrodes. An example is given in Fig. 1.1, which will be explained later on.

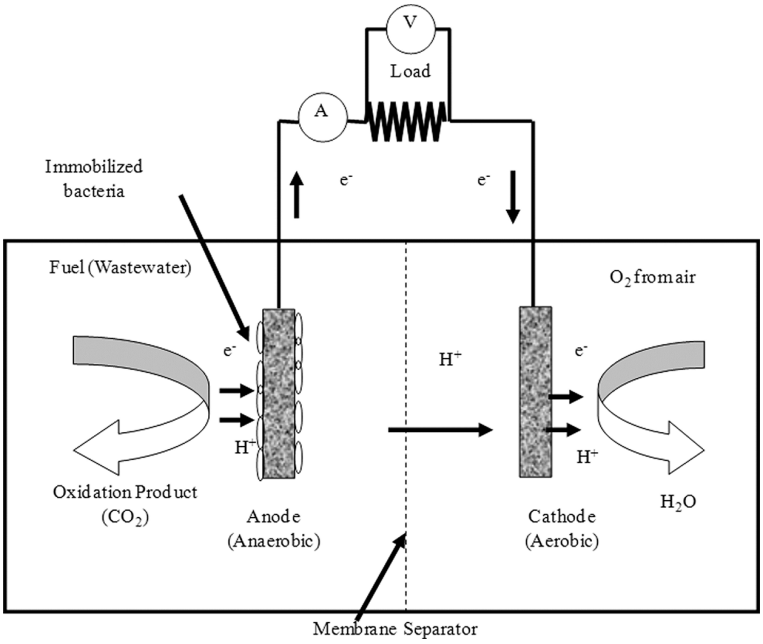

Figure 1.1: Example of a two-chamber MFC [4, p. 2]

In nature a variety of bacteria and compounds are available for MFCs; the combination of these can improve the performance of the system. In recent decades a variety of efficient MFC systems were produced and in 2018 Mohan et. al [5] gave a comprehensive overview of MFCs. A huge benefit of MFCs is the treatment of wastewater; the bacteria used in MFCs utilise a wide range of (in)organic compounds to feed their activity. In other words, the microbes remediate wastewater in a natural way [6]. However, this master's thesis focuses only on the electrical power generation and tries to correlate the improvements of materials and configurations on the electricity production.

1.2 Problem statement

Due to climate change and the growing need for energy, it is necessary to shift power generation towards renewable and environmentally friendly sources. Recent studies have shown that specific bacteria like Geobacter sulfurreducens or Shewanella oneidensis can generate electricity while feeding on organic waste and aquatic sediments [2]–[5]. Although their electricity output is very small yet, the technology can help providing a sustainable source of energy and the bacteria can play a role in wastewater remediation. These bacteria live in anaerobic conditions underground, such as the bottom of streams and ponds or underneath water plants. These plants are capable of feeding the bacteria through their roots to provide continuous nutrition. It is possible to take advantage of the abilities of these bacteria; a plant MFC (PMFC) system sustains the bacteria with nutrients from plants, and is able to harvest electrical power from the same bacteria. The plants are not necessary to perpetuate the working principles of the system, but they provide a way to implement a more natural MFC. One of the advantages of (P)MFCs is that they can operate during day and night, although the power output declines during the night [6],[7]. Therefore, it is an interesting system to use in open air if there is enough daylight.

Another expanding problem is the large energy and material demand of wastewater treatment [8], [9]. There are more than 22 000 wastewater treatment plants in Europe, which use more than 1% of the Europe's total energy consumption. Therefore, it is recommended to obtain more energy-efficient and renewable ways to remediate wastewater. Different research groups all over the world are searching for solutions to the problems stated above. One of the most promising technologies at the moment are Constructed Wetlands. In this technology, manmade ponds filter wastewater naturally using a combination of aquatic plants and bacteria [10]–[12]. There are many different configurations, such as Up Flow-, Down Flow constructed wetlands (CWs) or a series of different scaled CW (stacked systems) [13]. When the wastewater treatment is combined with Microbial Electrochemical Technologies (MET) for energy harvesting, the system is called METland [14], [15]. The overall efficiency of the wastewater remediation is promising, but more research is needed since there is a variety in systems and power outputs. Especially when the relatively small setups are upscaled, the overall efficiency decreases. The X-LAB group at Hasselt University is investigating methods to produce electricity and treat wastewater with microbial fuel cell technologies like (P)MFCs and METlands, and their overall goal is to develop more efficient MET systems. The research of this thesis will be an addition to the ongoing activities of X-LAB.

1.3 Objectives

The general objective of this work is to obtain a better understanding of the relation between the geometrical configuration (architecture, dimensions,..) of MFCs and the corresponding electrical output in order to obtain design rules for an appropriate upscale engineering. The approach followed in this work is to define a matrix of test MFC systems with a variation of dimensional parameters (e.g. radius/volume) and to perform a systematic electrical characterisation in order to obtain the aimed design/output relations.

A first activity is a literature study which aims to provide an overview of the current know-how on MFCs. The systems have to be investigated and together with the existing knowledge, every part in the system will be taken into account before proceeding further. The building blocks (electrodes, bacteria species, nutrition, etc.) in the system will be studied towards a maximum power output. The next goal is to characterise the MFCs by comparing the acquired knowledge from the literature with fits in ZView. A main part of this goal is to investigate the influence of electrode area and surface/volume-ratio to the electrical power output of a PMFC. First the impedance of the system, together with the polarization curves have to be determined. The influence of scale and surface area of the electrodes to the impedance has to be fitted and analysed. Afterwards, the knowledge of the small scaled system can be used to create a design for a larger MFC with optimal electricity output. Before the COVID-19 crisis an additional goal was to monitor existing H-cells and mudd-based MFC prototypes available at X-LAB. However, access to the facility is denied for all students and experiments can not be executed. Therefore, a protocol is written as a roadmap for executing the experiments like they should have been performed. The protocol consists of the H-cell experiment on one hand and the Sediment MFC (SMFC) experiments on the other hand. The aforementioned fits of the system should replace the building and measuring stage.

1.4 Research outlook

First the basics and working principles of different configured MFC systems are explained. Afterwards the chapter discusses the measuring techniques that are commonly used to measure the performance and the internal resistances of MFCs. Techniques and materials that can improve the electrical power output are elucidated, as are the problems with upscaling. Subsequently a design of experiments (DOE) illustrates a method and setup to measure the influence of the electrical power output in function of the electrode radius/volume, which was the original goal of this master's thesis (before COVID-19).

The results consist of different protocols as a roadmap for executing the experiments like they should have been performed. The protocol consists of the H-cell experiment on one hand and the SMFC experiments on the other hand (MudWatt). Afterwards EIS fits of MFCs replace the building and measuring stage. Finally a discussion and conclusion will critically review the results and explain the findings and the further research that is needed.

Chapter 2

Materials and methods

2.1 Microbial Fuel Cells

2.1.1 Working principle

MFCs can be configured in many ways. A two-chamber MFC, which was previously shown in Fig. 1.1, is an artificial system with the purpose of maximising the electrical power output [4]. The cathode chamber is an aquatic environment with, in this example, some of the area in contact with air. The cathode itself is set up in a way that it is in contact both with water and air. The anode chamber is air-tight and contains an aquatic solution with anaerobic bacteria. The environment of the bacteria needs in general to be anaerobic because the majority of organisms cannot survive if the oxygen levels are above 10% [7]. The bacteria attach as close as possible to the anode. Protons are generated when organic fuel is oxidised by the bacteria. Subsequently they diffuse through a specific membrane separating the two chambers to the cathode. Due to the lack of oxygen in the anode chamber, the bacteria need another electron acceptor. An external conducting circuit empowers the electrons to generate a current via the external circuit from anode to cathode.

As an example, acetic acid in the aquatic solution at the anode is reduced by the bacteria to carbon dioxide (CO_2):

$$C_2H_4O_2 + 2H_2O \quad \rightarrow \quad 2CO_2 + 8H^+ + 8e^- \tag{2.1}$$

The protons diffuse through the membrane separating the two chambers, while the electrons generate the current from anode to cathode via the external circuit. Finally, oxygen is available at the cathode to combine with the electrons and protons to produce water.

$$2O_2 + 8H^+ + 8e^- \quad \rightarrow \quad 4H_2O \tag{2.2}$$

It is possible to combine the two electrode compartments in a one-chamber MFC. The anaerobic and aerobic compartment are both necessary to operate in the correct way. In this case they are taken together in a single chamber (Fig. 2.1), which is why the name single chamber MFC is self explanatory. The working principle is similar to that of a two chamber MFC, with the difference that the proton and electron flow is (in most single chamber MFCs) vertical like the

figure shows. For example, a sediment MFC is a natural system in which the aerobic cathode lies on top of the vertical system and is in contact with air. The anode is still anaerobic under a layer of natural sediment. The bacteria cannot survive long periods of drought, which is why the anode needs to be aquatic. Another benefit of making the system more aquatic is that it facilitates the attachment of bacteria to the anode and the diffusion of protons from anode to cathode [8].

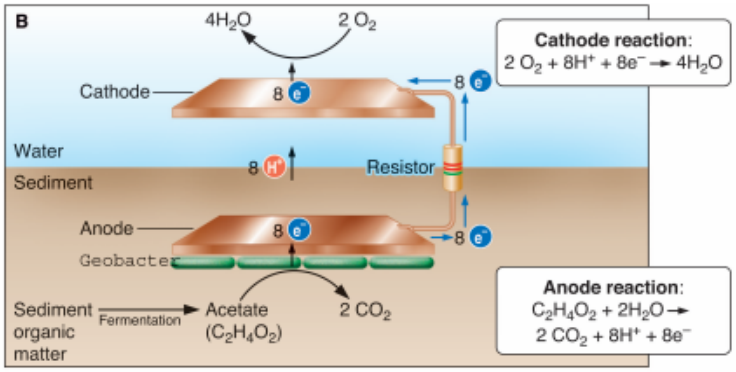

Figure 2.1: Example of a sediment MFC [9, p. 324]

The main difference between the two and one-chamber MFC is the separating membrane. The lack of efficient proton separator in a sediment MFC results in a lower voltage difference between anode and cathode. However, the difference in pH-values between top and bottom of the system is still the driving force behind the diffusion of protons.

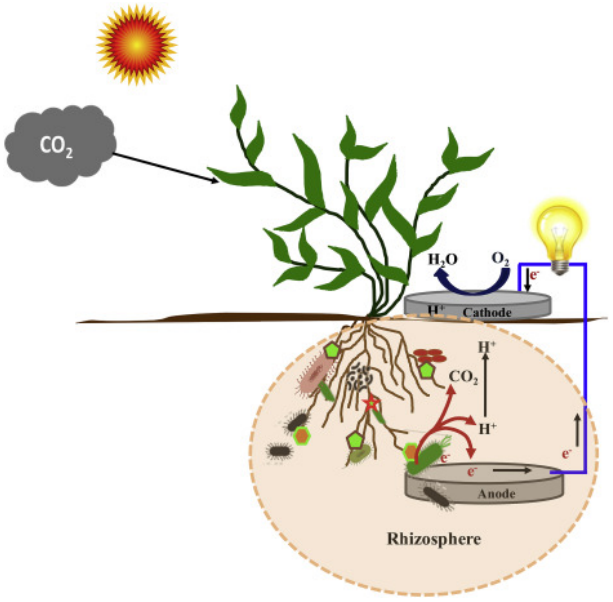

Figure 2.2: Example of a PMFC [5, p. 554]

Since an MFC is an artificial laboratory system, integration in the environment could be optimised by using more natural resources. The bacteria used in an MFC only need nutrition that they can reduce to guarantee the working of the system. A plant microbial fuel cell is a system which combines MFCs with plants along the cathode. An example is given in Fig. 2.2. The advantage of a PMFC over a classical MFC is that they run mediator free [5]. Plants harvest light energy to convert CO_2 to carbohydrates. The plants transport the carbohydrates to their roots where they

are released into the rhizosphere (the small soil region directly influenced by the plants' roots). The nutrients released in the rhizosphere diffuse to nearby soil which contains aforementioned bacteria. This process is not only beneficial for the bacteria but also for the soil environment, since bacteria reduce these nutrients to a consumable form, after which the nutrients can be absorbed again by the roots of the plants. The whole rhizosphere benefits from this process when containing a healthy microenvironment.

In a natural symbiosis between bacteria and plant in the rhizoshpere, the electrons liberated from the bacteria consumption are lost in the rhizoshpere soil. Therefore, it is possible to harvest the electrons with an external circuit. The system functions as a sediment MFC with a plant suitable for this system along the open-air cathode. The anode with micro-organisms is placed next to plants rhizosphere for optimal electron harvesting. The electrons move from anode to cathode via the external circuit like in a sediment MFC. One of the advantages of PMFCs is that they can operate during day and night, although the power output declines during the night [10, 11]. Therefore, it is an interesting system to use in open air provided there is enough daylight.

2.1.2 Electron transport mechanisms

Diverse families, genera and species of bacteria are used to assure the operation of an MFC. The most commonly of genus is the *Geobacter*, a fortiori *Geobacter sulfurreducens* [8, 9, 12]. Another commonly used genus is the *Shewanella*, more specifically *Shewanella oneidensis* [13]. There also were successful experiments with lots of other bacteria species (e.g. *Desulfuromonas acetoxidans*, *Aeromonas hydrophila*, *Thodoferax*, ...) but in general the former two are used.

The aforementioned bacterial species attach in normal circumstances directly to the anode and use extracellular electron transport. This first electron transport mechanism is called 'direct contact'. However, different extracellular electron transfer mechanisms exist, such as electron shuttles and nanowires for G. Sulfurreducens and S. Oneidensis. A representation of the different mediator mechanisms is given in Fig. 2.3.(**C**) and (**D**).

The second electron transport mechanism utilises artificial mediators. These are electron shuttles who transport electrons from inside the cell throughout the cell membrane to the anode. The electron shuttles consist of certain proteins and load themselves with e.g. an electron in the organism. Thereafter they unload the electron at the anode, after which they penetrate the cell membrane again [14]. An example of such an entity is *Proteus vulgaris*, who oxidises sucrose to carbon dioxide and the electrons are shuttled to the anode by thionine as a mediator [15]. The mediators are important in MFCs using micro-organisms such as *Escherichia coli* or *Pseudomonas*. There are micro-organisms who produce their own mediators like *Shewanella oneidensis*.

A third mechanism used to raise the power output is the existence of bacterial nanowires. These small long structures (10nm diametre) go through the cell membrane and conduct e.g. Fe^{3+}-oxide. Bacteria close to the anode enlarge the conducting surface using nanowires. Especially the *Geobacter sulfurreducens* species makes a conductive network of nanowires, which is captured by Gorby et. al [17] in Fig. 2.3.**A**. This network attaches itself to the anode as one large conductive network of electron donors and consequently increases the power density of the system. The term nanowire is also used for a conductive appendage; an extension of the outer membrane of the bacteria cell [19]. An example is given in Fig. 2.3.**B**, which shows different S. Oneidensis bacteria

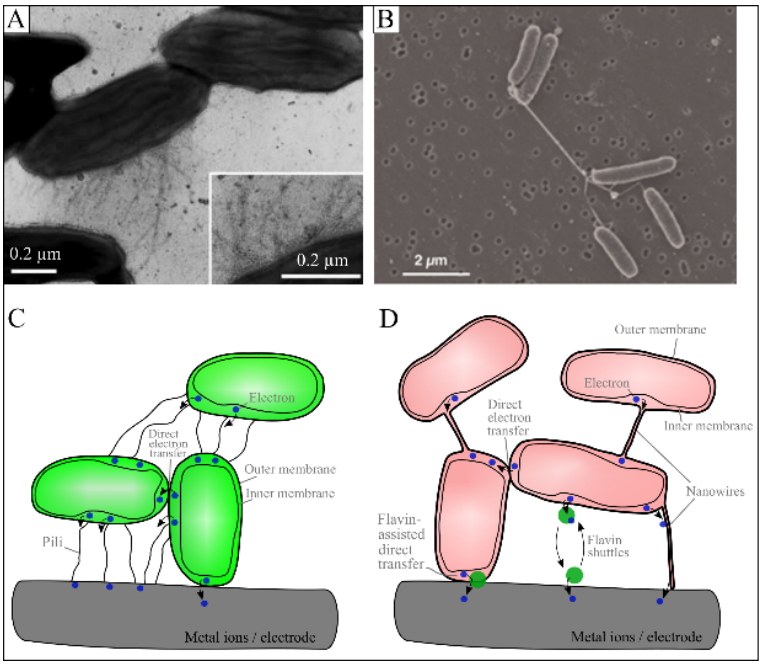

Figure 2.3: Extracellular electron transfer mechanisms of the *Geobacter Sulfurreducens* and *Shewanella oneidensis* bacteria. (**A.**) gives two G. Sulfurreducens bacteria and a conductive network of bacterial nanowires [16, p. 1099]. (**B.**) are multiple S. Oneidensis bacteria which are connected through nanowires [17, p. 11359]. (**C.**) and (**D.**) represent extracellular electron transport pathways for G. Sulfurreducens respectively S. Oneidensis [18, p. 10]

connected by nanowires. Like the G. Sulfurreducens uses a conductive network, S. Oneidensis can create a conductive network of nanowires which attaches to the anode in a similar way (the differences lead too far). In that way the power density can rise because one large conductive network of electron donors is made.

2.2 Measuring techniques

To evaluate the electricity outcome of an MFC, different parameters and techniques are used. The electricity output and the wastewater treatment can be evaluated with the electrode electrical potential, the power density and the energy efficiency. These parameters are obtained from measurements like chronoamperometry, EIS and cyclic voltammetry, done with a potentiostat. Afterwards they can be used to plot polarization and power density curves. This section focuses on the main parameters and techniques used for MFCs [20, 21].

2.2.1 Performance parameters

The 'electrical potential of the electrodes' is a self-explanatory term and is measured in voltage. It is compared to a reference electrode, because it is a relative value and thus needs some kind of calibration. Different reference electrodes can be used such as Ag/AgCl, standard hydrogen electrode (SHE) and saturated calomel electrode (SCE). The different reference potentials are dependent on pH and can be found in datasheets.

An important parameter to compare different MFCs is the power density: the amount of power the system can deliver per area or volume. Since the bacteria attach to the anode, the area of the anode is often used to project the surface area. The power density is therefore calculated as:

$$P_{anode} = \frac{E_{cell}^2}{A_{anode} R_{Ext}}, \quad \left[\frac{W}{m^2}\right] \tag{2.3}$$

where R_{Ext} represents the external resistance and A_{anode} is the surface area of the anode. E_{cell} is the measured cell voltage defined as

$$E_{cell} = V_{OC} - IR_{int}, \tag{2.4}$$

in other words the cells open circuit voltage (V_{OC}) minus the sum of all the internal losses of the MFC [20]. It is also possible to investigate the power density using the cathode surface area instead of the anode, but this method is less common. Sometimes it is difficult to calculate the surface area of the anode or the cathode reaction limits the overall power generation. Consequently the previous definition of power density is less preferable and the parameters of the cathode should be used instead of the anode parameters.

To compare MFCs with other fuel cells, it is suggested that the power density is normalised to the total reactor volume V instead of the area:

$$P_v = \frac{E_{cell}^2}{v R_{ext}}, \quad \left[\frac{W}{m^3}\right] \tag{2.5}$$

However, it is hard to compare different MFC configurations (single or dual chamber). Alternatively the total anodic compartment volume could be used as parameter instead of total reactor volume. In stacked systems the cathode air-space volume should be included in the total reactor volume.

Another parameter is the overal energetic efficiency and is defined as the power produced by an

MFC devided by heat of combustion of the organic substrate over a timeframe t:

$$\epsilon_E = \frac{\int_0^t E_{cell} I dt}{\Delta H m_{added}} \tag{2.6}$$

I is the current $\left[\mathrm{A}\right]$, ΔH the heat of combustion $\left[\frac{\mathrm{J}}{\mathrm{mol}}\right]$ and m_{added} the amount of substrate added $\left[mol\right]$. The energy efficiency is used to evaluate the energy recovery of an MFC and has a range from 2% till 50% [20]. The energy efficiency is mainly calculated for influents with known compositions, since the heat of combustion is not known for all kinds of wastewater. However, it is difficult to measure the energy efficiency for different configurations of MFCs. This is because different scaled systems with exactly the same parameters differ in energy efficiency. Therefore, power density is more commonly used, although in this case it is different to compare the 2D with 3D systems. A golden standard to measure energy efficiency or to compare power densities is not known yet.

2.2.2 Current-voltage profile: polarization and power density curve

Typical plots to evaluate the performance of an MFC are polarization curves in combination with power density curves [20, 22]. The plots give an indication of the performance of the anode, cathode and/or the total MFC. A polarization curve plots the cells electrical potential in function of the current density (Fig. 2.4.a). The power density curve (Fig. 2.4.b) visualises the maximum power point (MPP) reached by a specific resistance. The internal resistance can be calculated from the slope of the plot.

Polarization curves are acquired by a potentiostat, different options exist for the polarization discharge curves [23]. First it is possible to periodically decrease the load while the voltage is measured. It is possible to use galvanostatic discharge, a method where the current is controlled and the voltage is measured. Potentio-dynamic polarization is a technique that uses linear sweep voltammetry (cyclic voltammetry), where the current is measured with a slow voltage scan rate, e.g. $1 - 50\frac{\mathrm{mV}}{\mathrm{s}}$. Finally potentiostatic discharge is a technique in where the voltage is controlled and the current is measured. For bio-electrochemical or MET systems the most suitable option is the latter; the constant potential (potentiostatic) discharge technique. In this two electrode method the working electrode is either anode or cathode, while the other serves as the counter electrodes. The current is calculated using Ohms law:

$$V = IR. \tag{2.7}$$

Three different zones can be distinguished in a polarization curve (e.g. Fig. 2.4):

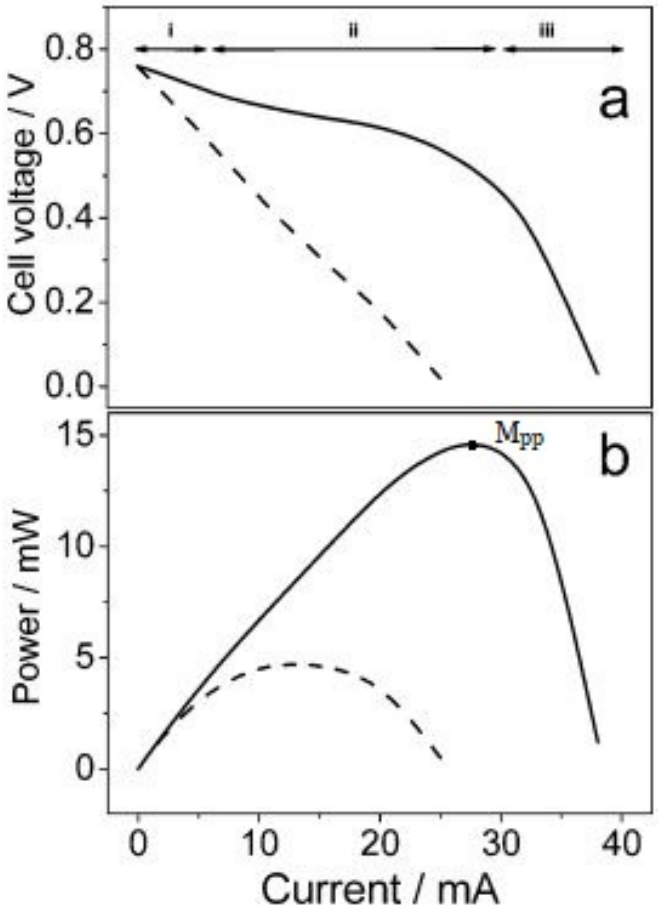

Figure 2.4: Example of a polarization (a) and power density curve with maximum power point (b). The dotted line fits the theoretical values, while the continuous line symbolises a measurement [20, p. 5188]

Zone (i): activation losses. The first zone starts from the V_{OC}, in other words the maximum electrical potential (E_{emf}) and decreases steeply. Activation losses are dominant in this region due to the slowness of the system. The charge overpotentials, which are the differences in reduction potential and the potential of the redox event, result from the reactions at open load and happen at the anodes surface. The concentration of protons close to the anodes surface is similar to that in the bulk solution.

Zone (ii): ohmic losses. The curve decreases slower than in zone (i); the voltage drop is almost linear with current. In this zone the ohmic losses are dominant due to ionic resistances in the MFCs electrolyte, biofilm and proton exchange membrane (PEM) due to the low ionic concentrations.

Zone (iii): concentration losses. The curve has a rapidly falling voltage when higher currents need to be delivered. In this region the concentration of reactants and products get unbalanced. In short, the bacteria are unable to deliver the reactants to the electrode reaction zones at the rate it is required to sustain the high current generation. Concentration losses are dominant in this zone because of the mass transport effects. The main imbalance happens between the anodes surface region and the bulk electrolyte, which can lead to reduction of reactants transport to where they are required.

The total internal resistance R_{int} can be obtained from the polarization curve, by calculating the slope of the linear curve in (ii) ($R_{int} = \frac{-\Delta \mathrm{E}}{\Delta \mathrm{I}}$) [20]. When the polarization curve is not linear, the use of electrical impedance spectroscopy (EIS) is preferred. In this case R_{int} cannot be defined, alternatively the ohmic resistance R_Ω and the electrode overpotentials can be measured with EIS.

Power curves are calculated from the polarization curve and plot power in function of current. From Fig. 2.4(b) it is clear that in an open circuit no power is produced. When the load increases the power increases until the MPP is reached. After the MPP, the power drops significantly until the resistance is too high to overcome by the electrical potential and no more power is produced. The MPP will typically occur when $R_{int} = R_{ext}$.

It is important to note that obtaining a steady state polarization curve with an MFC is difficult [23]. The nature of the species evolves with time, causing the electroactive metabolites, biofilm- and catalyst structure to change constantly. Different types of MFCs require different sampling rates.

2.2.3 Electrical Impedance Spectroscopy

This technique is used to study the electron transfer characteristics at both anode and cathode, since they play mayor roles in the overall performance of an MFC [24, 25, 26]. The goal is to acquire the different electrical components of the MFC system, to develop an equivalent circuit model (ECM). This consists of a combination of resistors and capacitors, which are discussed later on.

EIS is usually done by a potentiostat, equipped with a frequency response analyser in three-electrode configuration [27]. To visualise the setup, consider e.g. Fig. 2.8, which will be discussed later on. There is one reference electrode, one counter electrode and one working electrode. The working electrode is attached to either the anode or the cathode, while the other serves as the

counter electrode. The reference electrode is plugged into the bottom hole in the figure, since there has to be a significant distance between the counter electrode and the reference electrode. With the reference electrode it is possible to control the voltage applied to the working electrode. This configuration allows to examine the performance of an individual electrode (working electrode). If the whole system needs to by analysed, another method should be used which only uses two electrodes. In this method the counter electrode serves as the reference electrode. However, the EIS data becomes more complicated due to more active processes at both the anode and cathode.

An AC signal perturbation with an amplitude of a few mV is imposed on the working electrode, while the frequency is varied in small steps over a wide range. The frequency sweep is typically from 10^6Hz to 10^{-3}Hz. The small perturbations prevent damage to the biofilm attached to the anode and ensure that non-linear harmonic effects do not interfere with the data collection. The current response is measured during each step of the frequency sweep. The reason why measurements at high frequencies are performed first is because frequency is inversely proportional to time. This means that high frequency data points are acquired fast. When the frequency lowers, the time to measure the current increases. If any damage would be done on the system during the measurement, the data already gathered at high frequencies is maintained (the majority of the data points). This would not be the case if the frequency sweep is done from low to high frequencies, since the lowest frequencies takes the most time to measure. Before the representation of data is discussed, a short explanation of the systems impedance is given.

When the electrodes are connected to an external circuit, the system will have a certain resistance-, inductance- or capacitance-character, which forms the system's impedance. The impedance consists mainly of ohmic resistances like contact resistances, wires, electrolyte, membrane, ... Contacts between e.g. wires and pincers are never ideal and can be represented as small capacitors [28]. The different impedances are all in series and therefore:

$$Z_{total} = Z_1 + Z_2 + Z_3 + \dots \tag{2.8}$$

Certain bacteria, with or without nanowires, are connected to the anode and will have a small capacitive effect. All the bacteria are connected in parallel, in such a way that:

$$\frac{1}{Z_{total,bacteria}} = \frac{1}{Z_1} + \frac{1}{Z_2} + \frac{1}{Z_3} + \dots \tag{2.9}$$

The capacitance of the connected bacteria to the anode are very small. For this reason, $\frac{1}{Z_{total,bacteria}}$ will be large and $Z_{total,bacteria}$ small. The latter is connected in series with the external circuit and should be summed like in 2.8.

When the electrical circuit elements are analysed, they can be fitted into an equivalent model. Resistors, inductors and capacitors can be modelled as follows:

$$Z_R = R \tag{2.10}$$

$$Z_L = j\omega L \tag{2.11}$$

$$Z_C = \frac{1}{j\omega C} \tag{2.12}$$

In an ideal resistor, the impedance is purely real and the current through this resistor is in phase with the voltage across it. In contrast, in an ideal inductor or capacitor the impedance is purely imaginary. The impedance of a capacitor decreases when the frequency increases and the impedance of an inductor increases in the same case. The impedance of an MFC consists mainly of resistors and capacitors, either in series and/or in parallel connection. The magnitude of the systems total impedance can be expressed in terms of real and imaginary components:

$$|Z| = \sqrt{Z_{real}^2 + Z_{imaginary}^2} \tag{2.13}$$

The phase angle of this complex impedance can be expressed as:

$$\Theta = tan^{-1}\left(\frac{Z_{imaginary}}{Z_{real}}\right) \tag{2.14}$$

Like previously mentioned, EIS uses an AC current of a few mV in order to obtain the impedance and phase angle of the system at that frequency. A commonly way used to represent the data are Bode and Nyquist plots [29], e.g. in Fig. 2.5. A Bode plot consists of two parts, the (absolute value of the) impedance and the phase angle, which are both plotted in function of the frequency on a logarithmic scale. In a Nyquist plot, each point represents the impedance at a given frequency, plotted in a complex plane.

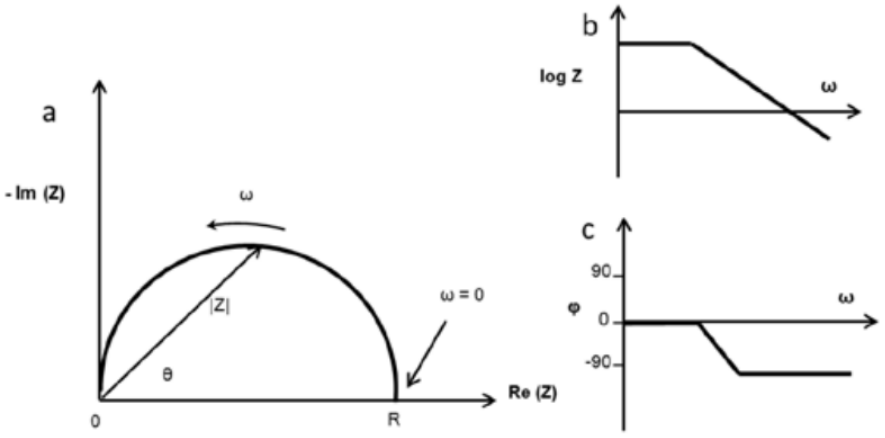

Figure 2.5: Example of a Nyquist plot (a) and Bode plots (b,c) [30, p. 1950]

When the Bode and Nyquist plots are fitted, an accurate equivalent circuit model can be developed, although this is a challenging task. The electrical equivalent of the system can describe the electrochemical phenomenons in the system via these representative models. This is the key to understand the performance and limiting factors of MFCs. Nyquist plots are used to obtain the charge transfer resistance (R_{rc}) of the different electrodes. Lower R_{rc} values result in larger charge transport from electrolyte to electrode and vice versa. To lower this resistance improvements like scientific adaptations can be made. The internal resistance of an MFC is the most important factor for power density and can be determined with EIS as well. An equivalent scheme for MFCs is, according to [30], a small extension of a Randles circuit (Fig. 2.6).

The R-values are the different ohmic resistances like contact resistances, wires, electrolyte, membrane, ... Contacts between e.g. wires and pincers are never ideal and can be represented as small capacitors [28]. Therefore, constant phase elements (CPE) are introduced which substitute

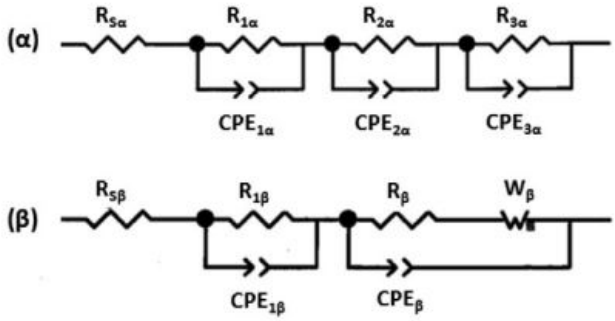

Figure 2.6: Equivalent circuits for (α) the global MFC and anode and (β) the cathode [25, p. 205]

these capacitors. The CPE also take into account actual surfaces like roughness, coating and the inhomogeneous solutions [31]. For the cathodic part value W is included to represent a generalised finite Warburg element which represents the models diffusion process resistance. Strik et al. 2008 and Zhao et al. 2009 emphasize the importance of stable operating conditions in order to obtain a correct equivalent circuit model (ECM) [23, 32]. Identifying the correct configuration of the electrical components in the circuit is the hardest task in EIS analysis.

A recent study of Rossi and Logan showed that the electrode size in H-cells (a specific type of two-chamber MFCs) has less influence than generally accepted [33]. EIS is mainly done to investigate the internal resistances of the system, which turned out to be more than 77% depending on the length and area of the tube connecting the anodic and cathodic chamber (neglecting any contribution from membrane or solution in the bottle). Rossi and Logan state that the electrode area in H-cells should be larger than the tube area to avoid diminished electrical power output in MFCs due to mass-transfer limitations and to minimise electrode resistances. Therefore, it is important to report the area and length of the tube connecting the H-cells when executing this protocol. Anode size influences the system heavily when smaller than the tube crossectional area (in this study $R_{Anode} = 26 \pm 1\Omega$ to $R_{Anode} = 431 \pm 229\Omega$). The cathode size influences the electrical power output even more when the cathode size is smaller than the tube area ($R_{Cathode} = 61 \pm 5\Omega$ to $R_{Cathode} = 1246 \pm 805\Omega$ in this case). For this reason all parameters except electrode size should be kept constant while investigating this specific variable and the tube dimensions need to be listed carefully.

2.3 Materials and configurations

Different improvements can be made to enhance the electrical power output of an MFC. This includes material improvements, surface modifiers, separators, MFC configurations and multi-electrode systems. The components and possible improvements are explained. At the end of the section, examples of different MFCs give more insight in expected power densities.

2.3.1 Components

The anode is the core part of an MFC, because the bacteria attach to it. It is favourable for the power output if the surface is as large as possible, while the volume is as small as possible. Anode materials should be both highly conductive and harmless for bacteria. A widely used and affordable material with great surface to volume ratio is carbon felt [34, 35]. Non-carbon materials are not recommended because corrosion will lead to detrimental effects on the bacteria.

The cathode is the most critical component for electricity generation. Lots of losses are possible and need to be minimised, such as losses due to electrochemical reactions, charge transport and mass transfer processes that take place in the cathode. A conductive material, harmless for the bacteria and with great surface to volume ratio is carbon felt/paper/cloth. A graphite plate is also possible but is more expensive. The surface area of the cathode is even more important than the surface area of the anode. The power output rises significantly if the cathode surface area increases till a certain limit is reached. Although specific values of the limits are still unclear, it is known that after the limit the additional surface area becomes inefficient. In other words a bigger surface after the limit is reached does not contribute to additional power output. Studies suggest that in small scale systems, 11 times bigger surface area leads to 10 times higher power output [5]. The ohmic overpotential of the cathode represents the voltage loss to drive proton and electron transport processes. It is a combination of ionic and electronic resistances and includes the resistances from electrode, electrolytes and interconnections. Naturally a lower overpotential leads to a higher power output at the end of the process and there are several ways to do that:

- Certain catalysts are available to enhance the efficiency of the cathode conductivity, like Cobalt tetramethylphenylporphyrin, Cobalt-Iron-Nitrogen and platinum (expensive) [36, 37]. Noncatalysed cathodes may have a large overpotential during oxygen reduction reactions, leading to decreased power output. The presence of a catalyst is therefore desirable as it lowers cathodic reaction activation energy and increases the reaction rate;
- Cathodic Electron Acceptors (EA) are oxidants which have a high redox potential leading to lower cathodic activation overpotential. Examples of cathodic EA are ferricyanide, permanganate, persulfate and dichromate [38]. Notice that these EAs are unable to regenerate by oxidation with oxygen, which makes it more difficult to implement this enhancement in an ordinary MFC. It requires continuous replenishment, which is possible yet difficult in continuous flow MFCs;
- When the oxidant concentration (O_2) rises, the power density increases;
- Temperature can alter the power output of an MFC, because higher temperature leads to improvement of efficiency in the cathode [36] and improvement of the bacterial activity.

Electrode modification is an approach to improve the power output by improving the attachment of bacteria to the anode or to promote biofilm growth. There are three main approaches: the

first are surface treatments, more specifically ammonia treatment. This is an efficient method to benefit the surface charge of the anode, which will lead to the growth of current-generating biofilms and consequentially enlarges the anode surface. Second a chemical modification tries to encourage the presence of metal oxide, because it benefits the development of electricity-producing biofilm. This is done by immobilising metals, metal oxides or other active compounds on the anode. Last a heat and/or acid treatment removes impurities and/or to enhance the active site of the anode and the conductivity [39].

To prevent oxygen diffusion and prevent short circuit from cathode to anode, separators are used between the two electrodes. These proton-permeable barriers diminish the gaping between anode and cathode. The rate of proton transfer from anode to cathode through the separator is lower than the consumption of protons at the cathode. Therefore, it is required to use separators possessing high cation transfer properties. However, this rate difference results in a pH gradient: the pH of the anodic chamber lowers relative to the cathodic chamber. The stability and performance of the system decreases and the overall internal resistance of the cell increases. Absence of a separator reduces the coulombic efficiency (CE) [40]. Many different separators are available, like cation or anion exchange membranes, size-selective separators and ceramic separators.

2.3.2 Upscaling

As mentioned before, the conventional setup is the one-or two-chamber MFC. Nevertheless there are many other configurations possible with different characteristics.

A one chamber configuration (recall Fig. 2.1) requires only an anodic chamber while the cathode is directly in contact with air. These systems are preferred over others because they are easy to handle due to small volume. They have a simplified operation and no additional aeration options. The short electrode gives relatively high volumetric power densities. An example system is the sediment MFC explained above, which is an MFC without a PEM. The advantage of such a system is the low cost and high power density for a small volume. However, the CE is lower than equipped with a PEM. The sediment volume between the anode and the cathode has to be big enough, because the presence of oxygen at the anode will result in lower metabolic activity of the microbes [7].

Many different two-chambered (or double chamber) MFC designs were tested to examine a maximum volumetric power density. The maximum obtained according to Mohan et. al [5] is $500\frac{\mathrm{W}}{m^3}$, using a miniature design with a cross-sectional area of $2cm^2$ and a volume of 1.2mL. The presence of a PMFC would lead to higher power densities than a single chambered system, but the high internal resistances are disadvantageous. This for the reason that the energy used to pump the fluid through the anodic chamber is much greater than the power output for the system. Double chambered MFCs are difficult to scale up because the designs are more complex, larger in volume and the internal resistances are higher.

It is possible to make a combination of different MFC in a stacked system [41]. If a series of different MFCs is used, the overall current output increases. However, power output in a series connection is much lower than in a parallel connection [42]. A stack of multiple MFCs in series suffers from voltage reversal problems: it is possible that one or several cells reverse their polarity because of fuel starvation, resulting in decreased power generation. Therefore, it is more useful to

connect MFCs in parallel (or combination of series and parallel) configuration if power production is the goal [43]. Parallel connected MFCs are appropriate for high current densities and rapid substrate degradation.

The power density of a single chamber MFC increases significantly if the amount of electrode pairs increases. Multi-electrode systems use multiple anodes and/or cathodes that lead to a rise in power density when the electrode size of the single electrode would become large enough. In one study, four pairs of electrodes resulted in a threefold increase of power density, while a study by Ren et. al [44] with a hexagonal MFC design and 11 electrodes had increased maximum power density in comparison with other systems. In general it is justified to conclude that smaller systems relatively have higher power densities. It is possible to enhance the electrical power output for larger systems by using multiple electrodes.

One big challenge in MFCs is upscaling: power density does not increase proportional to bigger scales of systems, according to Winfield et. al [45]. Winfield suggested that efficient upscaling is possible by connecting multiple small MFC systems rather than one larger unit, which confirms that separating electrodes and stacking smaller MFCs in parallel is useful. It is not possible to compare different scaled MFCs, even if every parameter is e.g. doubled. The efficiency in MFC systems declines rapidly if they increase in size [46]. Note that most investigated MFCs in other research are smaller in such way that the electrode distance is minimised and the systems have effective PEMs. In large MFCs the PEMs are replaced due to the cost or the distance between the electrodes is increased which leads to a reduction of power output. This should be taken into account when comparing the electrical power output of different scaled MFCs. Further research is definitely needed regarding different upscaled MFC setups and combinations with large multielectrode MFCs. To increase the power output in an upscaled system, it is important to minimise the distance between the electrodes when separated by a PEM [47]. When a sediment MFC is used, incentives are given to increase the distance between the electrodes [48]. In the latter study 2 or 3 cm gives higher power density than only 1cm distance between the electrodes.

2.3.3 Examples

Table 2.1 shows a variety of different MFC systems together with their maximum constant power density output. Since a lot of different configurations, wastewater input, materials and separators are used, the power density differs significantly. Overall the power density rises with increasing number of MFCs used. Improvements in materials like platinum (which is highly conductive and does not harm the bacteria) result in higher power outputs. The presence of a separator and an aquatic environment between the two electrodes (hydrogen can diffuse more easily) are also beneficial to the system.

Table 2.1: Examples of maximum constant power densities and chemical oxygen demand (COD) removal in different MFC system setups.

Ref.	Configuration	Wastewater	Anode material	Separator	Cathode material	Power density
[49]	Single chamber MFC	Dairy	Graphite	Nafion-117	Graphite	$1.1 W/m^3$
[50]	Single chamber MFC	Dairy	Graphite-coated stainless steel mesh	PTFE	Carbon cloth	$20.2 W/m^3$
[51]	Single-chamber air-cathode MFC	Brewery	Carbon cloth	PTFE diffusing layer	Carbon cloth containing platinum	$0.528 W/m^2$
[52]	Serpintine-type MFC	Brewery	Graphite felt	-	Carbon cloth	$4.1 W/m^3$
[53]	Dual chamber MFC	Palm oil mill effluent	Carbon graphite	Nafion-115	Carbon graphite	$0.45126 W/m^2$
[54]	Dual chamber MFC	Domestic	Graphite granules	Earthen pot	Carbon fiber brush	$2.05 W/m^3$
[55]	Multi anode/ cathode MFC	Biomass from municipal plant	Graphite rods	-	Carbon cloth	$0.3 - 0.38 W/m^2$
[56]	Upflow MFC		Activated carbon fiber felt	PEM	Activated carbon fiber felt	$0.105 W/m^2$
[57]	Dual chamber MFC	Paracetamol	Graphite felts	Nafion-117	Graphite plates	$0.206 W/m^2$
[58]	Single chamber air-cathode MFC	Synthetic penicillin	Carbon felt	-	Platinum	$101.2 W/m^3$

2.4 Design of Experiments

Two different systems are built to investigate the performance of an MFC. First, H-cell MFCs available at X-lab are characterised by measuring the I-V characteristics and EIS. Later on different SMFCs are built to measure the effect of the electrode size on electrical power output.

Before the COVID-19 crisis, different setups of SMFCs were also designed and made. The setup is shown if Fig. 2.7. The goal of the experiment is to measure the I-V characteristics and the different internal resistances with respect to scale.

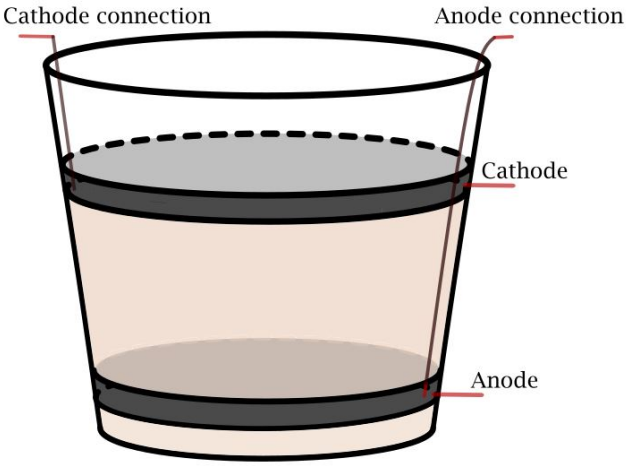

Figure 2.7: SMFC test matrix with varying volume and radius. The top electrode (gray) is the cathode, which is in direct contact with air. The bacteria in the sediment attach to the anode (gray) at the bottom.

The SMFC test setup consists of two carbon felt electrodes because it has great surface-to volume ratio and is harmless for electroactive bacteria. Stainless steel wires are used because the material is also harmless for the bacteria. The wires are provided with an insulation of heat-shrink tubing to prevent short-circuit current. The casing is a polyethylene bucket (with different scales of the same shape). The sediment between the electrodes was taken from the Stiemerbeek which flows along the buildings of Hasselt University. To improve the attachment of bacteria to the anode surface at the bottom, a small layer of sediment is placed under the anode. The SMFC experiment had two parts: the first setup consisted of different scaled systems with constant circular electrode thickness, constant sediment height and varying radius. The exact dimensions of the systems are shown in Table 2.2. The second setup had varying sediment filling and different scaled volume. The electrodes are circular shaped and varied in radius and in thickness. Table 2.3 shows the dimensions of the second setup.

Table 2.2: Design of SMFC test matrix with varying radius. Other parameters are kept constant.

System diameter (mm)	Ø 80	Ø 120	Ø 150	Ø 190	Ø 210	Ø 360	Ø 440
Cathode (mm)	15	15	15	15	15	15	15
Sediment (mm)	40	40	40	40	40	40	40
Anode (mm)	15	15	15	15	15	15	15
Sediment (mm)	10	10	10	10	10	10	10

For both experiments, seven different scaled systems are built from top diameter 80mm till 440mm. The height of the sediment, anode and cathode is constant in the first experiment

Table 2.3: Design of SMFC test matrix with varying volume. Other parameters are constant again.

System diameter (mm)	Ø 80	Ø 120	Ø 150	Ø 190	Ø 210	Ø 360	Ø 440
Cathode (mm)	5	10	15	20	20	25	30
Sediment (mm)	20	40	60	80	80	100	120
Anode (mm)	5	10	15	20	20	25	30
Sediment (mm)	5	10	15	20	20	25	30

to test the influence of radius on the electrical power output. In the second experiment the height of the electrodes and the sediment below the anode is the same. The sediment between the electrodes is four times this height. As the system increases in scale, the height between the sediment, anode and cathode varies with a constant factor (x2, x3, x4, x5, x6). This is to investigate the changes in electrical power output when the volume of the system diversifies. Due to the COVID-19 virus, the laboratory was unfortunately closed and the experiments could not be executed. Therefore, a next generation model of the latter experiments is elaborated in detail. The setup is shown in Fig. 2.8.

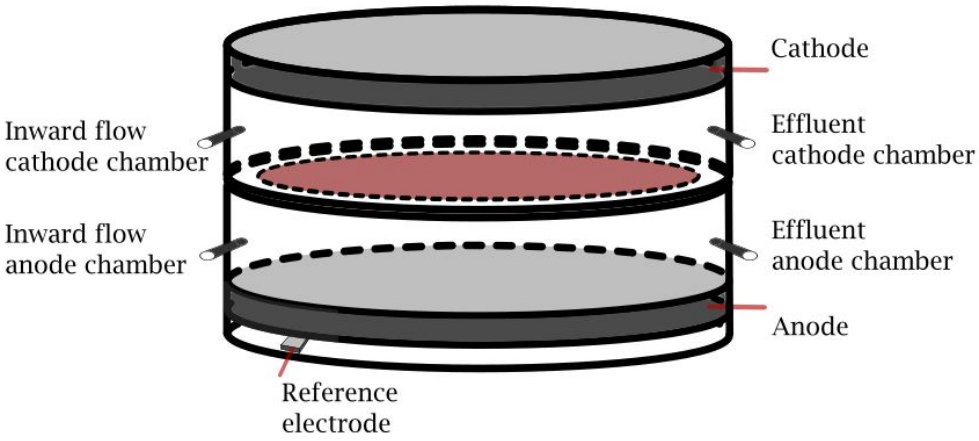

Figure 2.8: Design of Experiments: the proposed next generation test structure. The graphite cathode at the top is separated from the graphite anode at the bottom by a Nafion 117 membrane (red). The flow through systems control the composition of the aquatic solutions in both anode chamber (bottom) and cathode chamber (top).

The goal of the setup is the same: investigate the electrical power output while varying volume and radius. The experiments should be performed like the section 2.2.3 discusses. The working electrode is attached to either the anode or the cathode, while the other serves as the counter electrode. The reference electrode is plugged into the bottom hole in the figure, since there has to be a significant distance between the counter electrode and the reference electrode. With the reference electrode it is possible to control the voltage applied to the working electrode. This configuration allows to examine the performance of an individual electrode (working electrode). To control the nutrients and compounds in both anode-and cathode chamber two separated flow-through systems are added to the design. This is because the composition of the solutions in both chambers slightly alter during the working process. The flow systems allow the control of this problem [59] with typical flowrates of 1 to 50 $\frac{\text{mL}}{\text{h}}$ [60, 61].

Towards an improved microbial fuel cell setup, the following materials are preferred above others.

The bacteria cultures used in the different models should all be the same. *Geobacter Sulfurreducens*, *Shewnella Oneidensis* or any of the previously mentioned families are sufficient as long as they are homogeneously distributed over the different anode chambers of the different MFC setups. To enhance the bacteria growth and reduction processes, acetate is recommended that should be added to the anode chamber via the flow system in a constant concentration [62]. The anode material is platinum when the power output is maximised because it is the best conductive and bio compatible material for MFCs yet [63]. However, platinum is very expensive and can be replaced by carbon-based material only with little diminished power output. Therefore this setup uses graphite plate electrodes which are applicable for MFCs [39] Nafion 117 should be used as PEM since it has high proton conductive capabilities and is well known for it's application in MFCs [64]. Ghasemi et. al suggests that sulfonated polyether ether ketone (SPEEK) is more cost effective and has higher COD than Nafion 117 [65]. However, in this study the goal is to enhance the electrical power output as much as possible and Ghasemi acknowledges Nafion 117 is better for this purpose. The oxygen and/or acetate levels that could leak through the Nafion is negligible [66].

In this improved setup, the idea of the test matrices from tables 2.2 and 2.3 still fit. To obtain an empirical formula of the electrical power output, the systems dimensions should be doubled for different MFCs. Because the performance parameters do not respond linearly, extra experiments are added between the doubled dimension experiments like in Tables 2.4 and 2.5.

Table 2.4: Design of the proposed next generation setup test matrix with varying radius

System diameter (mm)	Ø 50	Ø 100	Ø 150	Ø 200	Ø 250	Ø 300	Ø 400	Ø 500
Cathode (mm)	5	5	5	5	5	5	5	5
Sediment (mm)	40	40	40	40	40	40	40	40
Anode (mm)	5	5	5	5	5	5	5	5
Sediment (mm)	5	5	5	5	5	5	5	5

Table 2.5: Design of the proposed next generation setup test matrix with varying volume

System diameter (mm)	Ø 50	Ø 100	Ø 150	Ø 200	Ø 250	Ø 300	Ø 400	Ø 500
Cathode (mm)	5	10	15	20	25	30	40	50
Sediment (mm)	20	40	60	80	100	150	200	250
Anode (mm)	5	10	15	20	25	30	40	50
Sediment (mm)	5	10	15	20	25	30	40	50

The experiments on the different scaled systems should all be performed the same. A detailed protocol is described in the chapter 3. At some experiments, the wastewater remediation is taken into account along the electrical power output. In that case, an additional optimised setup is attached in Appendix B.

Chapter 3

Results

First the protocols for the current-voltage profiles and the polarization curve is given. Afterwards the different EIS protocols are briefly discussed. Because it should be possible to detach these pages, some explanations are repeated between the measurements. Finally, fits on existing data of Ter Heijne et al. give more insight in the techniques of data analysis [67] .

3.1 Current-voltage profile measurement protocol

3.1.1 H-cell

Step 1: build the H-cell. Make sure that the different scaled systems are filled with the same homogeneous solution and the bacteria cultures are homogeneously distributed over the anode chambers. List all the dimensions and parameters of the system before proceeding.

Step 2: setting up the potentiostat. Different potentiostats that fit the right specs are available on the market, e.g. devices from *Keithley*, *Gamry*, *PalmSens*, ... At X-LAB the available potentiostat was the VersaSTAT 3F from *Ametek*. The V_{OC} needs to be known before starting the measurement. Therefore, connect the working electrode to the anode and the counter electrode to the cathode without external circuit. If the potentiostat needs a certain resistor value it has to be as high as possible (theoretically infinite). Measure the V_{OC}, typical values for H-cells are between 0.3 V and 1.1 V. Set up the potentiostat in such a way that it will sweep from V_{OC} to zero voltage.

Step 3: connecting the electrodes. The potentiostatic discharge method from section 2.2.2 should be used. The working electrode is attached to either the anode or the cathode, while the other serves as the counter electrode. This configuration is to analyse the polarization curve of the whole system. When only one electrode needs to be analysed, the counter electrode is not the anode or cathode. In that case, the counter electrode needs to be placed in the electrode chamber of the working electrode in the direction of the proton gradient (between anode and cathode). This is not included in the novel design because it complicates the setup heavily and the main resistances of the system should be analysed with EIS. Make sure every conductive connection is made flawlessly.

Step 4: start the current-voltage measurement. When running to the previous steps correctly, the potentiostat will enter the voltage and measure the current for every voltage. Make sure to keep

track of the different measurements over the different scaled systems (label every document).

Step 5: analyse the data. It is possible to create polarization curves by plotting the voltage vs. the current. The power is obtained by:

$$P = V \,.\, I \quad [W] \tag{3.1}$$

As mentioned in section 2.2.2 the three different zones in the polarization curve (Fig. 2.4) can give insight in the types of losses in the H-cell. Calculating the slope of the second part of the polarization curve gives the total internal resistance of the H-cell: $R_{int} = \frac{-\Delta E}{\Delta I}$ (only when the slope is linear, otherwise EIS is preferred). Finally, the power density curve is created by plotting the power vs. the current. The MPP occurs when $R_{int} = R_{ext}$, which is the optimal working point of the H-cell.

3.1.2 SMFC

Step 1: build the SMFC. Just as in the H-cell, make sure that the different scaled systems are filled with the same homogeneous sediment. In this case the mix of bacteria species are distributed in the same population percentages over the different anode chambers. It is possible to add a percentage of potting soil in case of sediment shortage, but it has to be minimised to enlarge the bacteria population per MFC. From bottom to top, there is first a small layer of sediment, subsequently the anode and a substantial amount of sediment that will act as PEM (dimensions in the DOE). The first small layer is to foster the attachment of bacteria to the anode (with or without nanowires). A stainless steel or titanium wire should run from to anode to the top of the system. It is necessary to put a heat-shrinking tube around the wire from the anode to the top of the system to prevent short circuit currents. The cathode at the top should be placed in a way that the water added to the SMFC nearly covers the whole electrode. List all the dimensions and parameters of the system before proceeding.

Step 2: setting up the potentiostat. Equivalent to the H-cell system different potentiostats fit the right specs. The experiment is similar to the H-cell experiment. First the V_{OC} needs to be known before starting the measurement. Connect the working electrode to the anode and the counter electrode to the cathode without external circuit. If the potentiostat needs a certain resistor value it has to be as high as possible (theoretically infinite). Typical V_{OC} voltages nowadays for SMFCs are between 0.8V and 1V (theoretically maximum at 1.14V [68]). Set up the potentiostat in such a way that it will sweep from the V_{OC} to zero voltage.

Step 3: connecting the electrodes. The potentiostatic discharge method from section 2.2.2 should be used. The working electrode is attached to either the anode or the cathode, while the other serves as the counter electrode. This is to analyse the polarization curve of the whole system. Because the counter electrode in an SMFC cannot be placed in the electrode chamber of the working electrode (single chamber MFC), analysing one electrode in an SMFC is not possible. Make sure every connection is made flawlessly.

Step 4: start the current-voltage measurement. When running to the previous steps correctly, the potentiostat will enter the voltage and measure the current at every data point. Make sure to keep track of the different measurements over the different scaled systems (label every document).

Step 5: analyse the data. It is possible to create polarization curves by plotting the voltage vs. the current. As previously mentioned in section 2.2.2, the three different zones (like in Fig. 2.4) can give insight in the types of losses of the SMFC. Calculating the slope of the second part of the polarization curve gives the total internal resistance of the SMFC: $R_{int} = \frac{-\Delta E}{\Delta I}$ (only when the slope is linear, otherwise EIS is preferred). The power density curves are calculated by plotting the power (Equation 3.1) vs. the current. Finally the MPP occurs when $R_{int} = R_{ext}$, which is the optimal working point of the SMFC.

3.2 Electrical Impedance Spectroscopy measurement protocol

3.2.1 H-cell

The EIS technique to use and connect the electrodes is comprehensively discussed in section 2.2.3.

Step 1: build the H-cell. Make sure that the different scaled systems are filled with the same homogeneous solution and the bacteria cultures are homogeneously distributed over the anode chambers. List all the dimensions of the system including the tube size.

Step 2: setting up the potentiostat. Many different potentiostats that fit the right specs are available on the market, e.g. devices from *Keithley*, *Gamry*, *PalmSens*, ... The half-cell potential of the anode biofilm needs to be known before starting the EIS measurement. Therefore, connect an external load of $200-1000\Omega$ to the system and measure potential versus the reference electrode. Make sure that every connection is made flawlessly. The value will be in range of millivolts.

Step 3: connecting the electrodes. As previously mentioned, the working electrode is attached to either the anode or the cathode, while the other serves as the counter electrode. The reference electrode has to be placed at a distance from counter electrode, at the opposite side of the working electrode. When the whole system needs to by analysed, the two-electrode method is used in which the reference electrode serves as the counter electrode (but the results in this configuration are rather complex and not recommended).

Step 4: start the measurement. Apply the measured AC potential to start the frequency sweep between working and counter electrode. Set up the frequency to sweep from 10^5 Hz to 10^{-3} Hz and start the measurement. The software delivered with the potentiostat will convert the measured current to a real and imaginary impedance at every data point.

Step 5: analyse the data. To create Bode plots, it is necessary to calculate the absolute impedance and the phase at every point of the measurement:

$$\begin{aligned} |Z| &= Z_{real}^2 + Z_{imaginary}^2 \\ Phase &= tan^{-1}\left(\frac{Z_{imaginary}}{Z_{real}}\right) \end{aligned} \tag{3.2}$$

After gain and phase are calculated, Bode plots can be produced by plotting the absolute impedance and phase vs. the frequency. A Nyquist plot is produced by plotting the real vs. the imaginary impedance.

3.2.2 SMFC

There is no tube or small cross-section in SMFCs that can prevent the optimal flow of protons to reach the cathode from the anode. Usually the sediment that acts as PEM has the same diameter as the circular electrodes. However, in every MFC experiment it is useful to list all the systems dimensions. For this reason it needs to be noted in the first step.

Step 1: build the SMFC. Like in the H-cell, make sure that the different scaled systems are filled with the same homogeneous sediment. In this case the mix of bacteria species are distributed in the same population percentages over the different anode chambers. It is possible to add a percentage of potting soil in case of sediment shortage, but it has to be minimised to enlarge the bacteria population per MFC. From bottom to top, there is first a small layer of sediment, subsequently the anode and substantial amount of sediment that will act as PEM. The first small layer is to foster the attachment of bacteria to the anode (with or without nanowires). A stainless steel or titanium wire should run from to anode to the top of the system. It is necessary to put a heat-shrinking tube around the wire from the anode to the top of the system to prevent short circuit currents. The cathode at the top should be placed in a way that the water added to the SMFC nearly covers the whole electrode.

Step 2: setting up the potentiostat. Equivalent to the H-cell system different potentiostats fit the right specs. Because there is no reference electrode in an SMFC the two electrode method should be used and only the total resistance of the system can be determined. Typical values to apply as AC potential in MFC systems for EIS measurements are between 1 mV and 10 mV. The internal resistances of an SMFC will be larger than this of an optimised artificial MFC. Therefore, the applied AC potential should be closer to 10 mV. It is possible that the AC potential needs to be higher than 10 mV. This occurs when the internal resistances of the system are very high, which means the current response is very small. Increasing AC potential should be done carefully and in small steps to prevent damaging the system.

Step 3: connecting the electrodes. The working electrode is attached to either the anode or the cathode, while the other serves as the counter electrode. The counter electrode serves also as the reference electrode in this configuration. Make sure that every connection is made flawlessly.

Step 4: start the measurement. Apply an AC potential of 10 mV to start the AC frequency sweep between working and counter electrode. Set up the frequency to sweep from 10^5 Hz to 10^{-3} Hz and start the measurement. The software delivered with the potentiostat will convert the measured current to a real and imaginary impedance at every data point.

Step 5: analyse the data. As described for the H-cell systems, Bode plots and Nyquist plots can be produced using the equations in 3.2 for all the different scaled SMFCs. Label the different fits with their system parameters to keep track of the MFC dimensions.

3.3 Fits

A dataset of Ter Heijne et al. from the paper "Analysis of bio-anode performance through electrochemical impedance spectroscopy" was kindly provided by the authors and is analysed in this section [67]. The influence of electrode size is not possible to investigate because the electrode size was constant during the measurements (and the electrode size was not published). The EIS frequency measurement as mentioned in the paper was done from 10 kHz to 2mHz with an AC perturbation of 10mV. However, the raw data received showed measured frequencies from 10MHz to 1.59mHz, but some data points are outliers so they were removed. Three united experiments were executed in this paper: first the acetate concentrations in the anode chamber are increased by steps (0mM, 1mM, 5mM, 20mM). Secondly, a phosphate buffer solution is added in different concentrations (0mM, 10mM, 20mM, 50mM, 100mM). It is this part of the experiment that will be analysed with fits. At last, the pH value is increased $(6, 7, 8)$. A picture and sketch of the setup is given in Fig. 3.1 a and b.

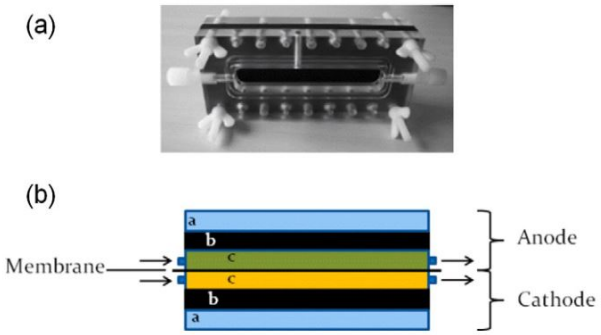

Figure 3.1: Setup of the experiments by Ter Heijne et al. In (a) a picture of a half cell with flow channel in front is given. (b) shows a schematic view of the whole cell with a. the plexiglas support, b. the Fumasep FTCM-E PEM and c. two separated flow compartments of anode (green) and cathode (yellow) [67, p. 65]

The support casing is made from plexiglas. The graphite plate electrodes are separated by a Fumasep FTCM-E exchange membrane. Both anode and cathode chamber solutions can be varied due to the separated flow compartments. The data from the first and second experiment is available and analysed with ZView. The electrodes are connected in three electrode configuration as described in section 2.2.3. The anode is the working electrode, the cathode the counter electrode and an Ag/AgCl reference electrode is placed in the anode compartment. Consequently this EIS setup will measure the electrical performance of the anode.

The buffer concentration was increased after the acetate concentration experiment. An example of a Nyquist plot analysed with raw data of the buffer concentration experiment is given in Fig. 3.2

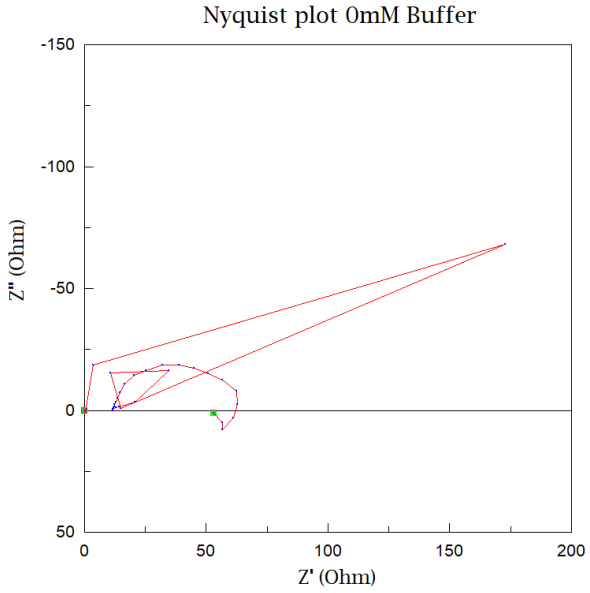

Figure 3.2: 20mM acetate 0mM buffer concentration complex plane plot of raw data produced in ZView with frequency sweep from 10 MHz (left) to 1.585mHz (bottom middle)

In normal EIS measurements on MFCs one or more semicircles as in Fig. 2.5 should be obtained. Therefore, it is clear that some outliers need to be removed from the raw data. At high frequencies (left) the system has not enough time to account for the changes is potential. At low frequencies the potential is disturbed by the slowness of the system and the changes in the biological activity at the anode. The adapted data sweep is done from 0.398 MHz to 2.512 mHz. The Nyquist plots for all the different bufferconcentrations are given in Fig. 3.3. The impedance and phase are calculated and represented in Bode plots in Fig. 3.4 for the different buffer concentrations.

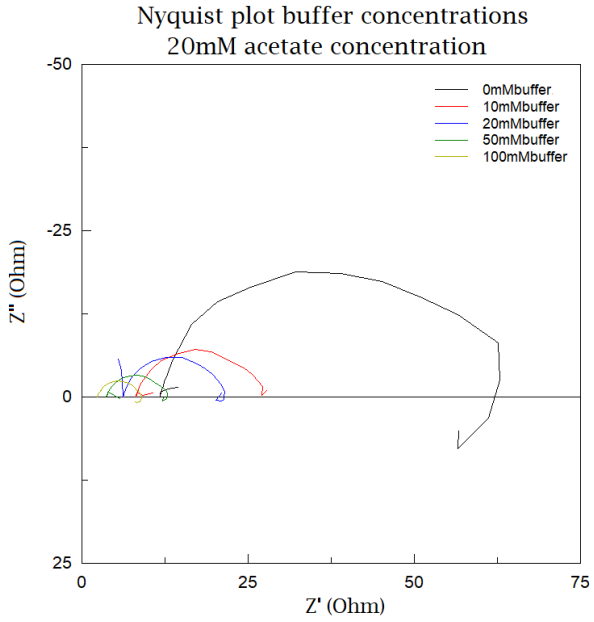

Figure 3.3: 20mM acetate concentration Nyquist plot with varying buffer concentrations, produced in ZView with frequency sweep from 0.398MHz to 2.512mHz

It is clear that the different phosphate bufferconcentrations influence the internal resistances of the system heavily. The Nyquist graph shows that higher bufferconcentrations lead to a reduction

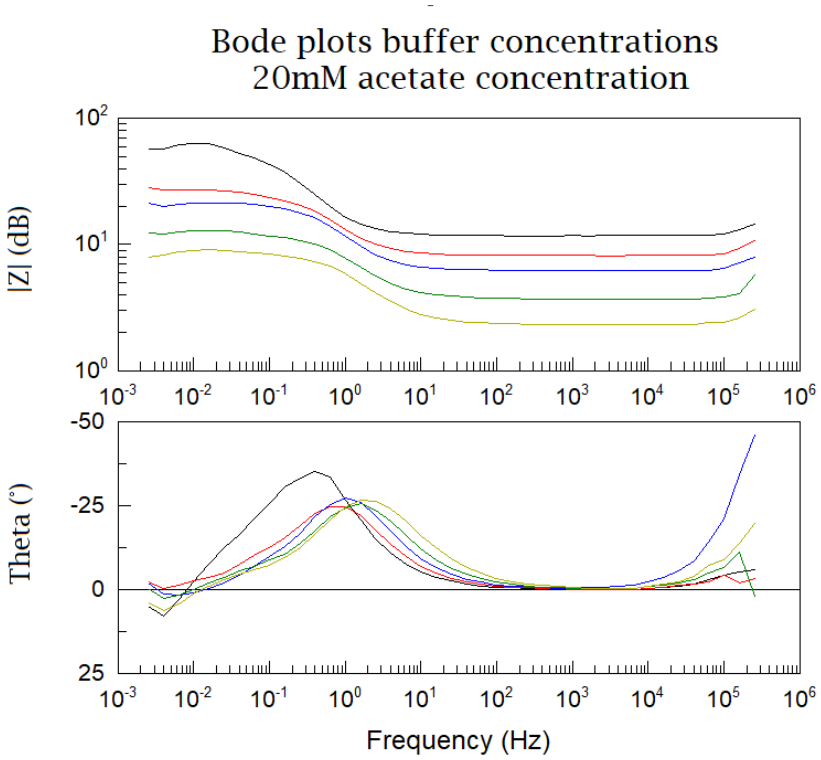

Figure 3.4: 20mM acetate concentration Bode plots with varying buffer concentrations, produced in ZView with frequency sweep from 0.398MHz to 2.512mHz

of the resistances in the system. The top of the Nyquist plot is reached when $\omega = 2\pi f = \frac{1}{RC}$ [29]. The Bode plots show the same result: higher buffer concentration leads to less impedance of the system and by consequence higher electrical power output. To get a better understanding of the resistances of the system, an EIS fit is made for different equivalent circuits of the anode chamber. This is done for the 0mM buffer concentration. Because the Nyquist plot of a RC-circuit is semicircular shaped a first fit with the corresponding equivalent circuit is shown in Fig. 3.5.

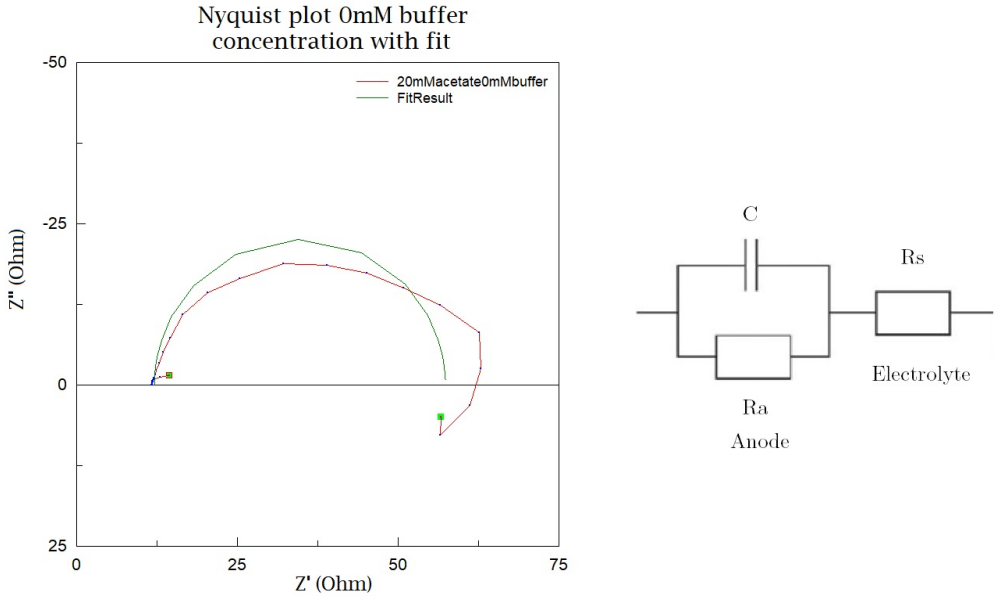

Figure 3.5: 20mM acetate 0mM buffer concentration Nyquist plot with fit (left) produced in ZView with frequency sweep from 0.398MHz to 2.512mHz and equivalent RC circuit (right) for the anode chamber. The capacitance and resistance of the anode are $0.02243 \pm 0.0009\mu F$ and $45.26 \pm 1.11\Omega$. The electrolyte resistance is $R_s = 12.12 \pm 0.14\Omega$.

The suggested ECM of Fig. 3.5 can be improved by changing the capacitor of the anode chamber by a CPE. As previously mentioned, CPE is used in place of a capacitor to compensate for non-homogeneity in the system, e.g. rough or porous surface leads to a double-layer capacitance to appear as a constant phase element with a CPE-P between 0.9 and 1. When CPE-P equals 1 than the equation is identical to that of a capacitor (phase angle of 90 degrees). CPE-T is related to the amount of carrier electrons on the MFC with different mechanisms such as diffusion and is expressed in μF. When the diffusion diminishes, it causes a decrease in CPE-T value, which improves the conductivity of the solution in the anode chamber [69]. The improved equivalent circuit for the whole system is suggested by He and Mansfeld [31]. The fit following this ECM is shown together with the ECM in Fig. 3.6.

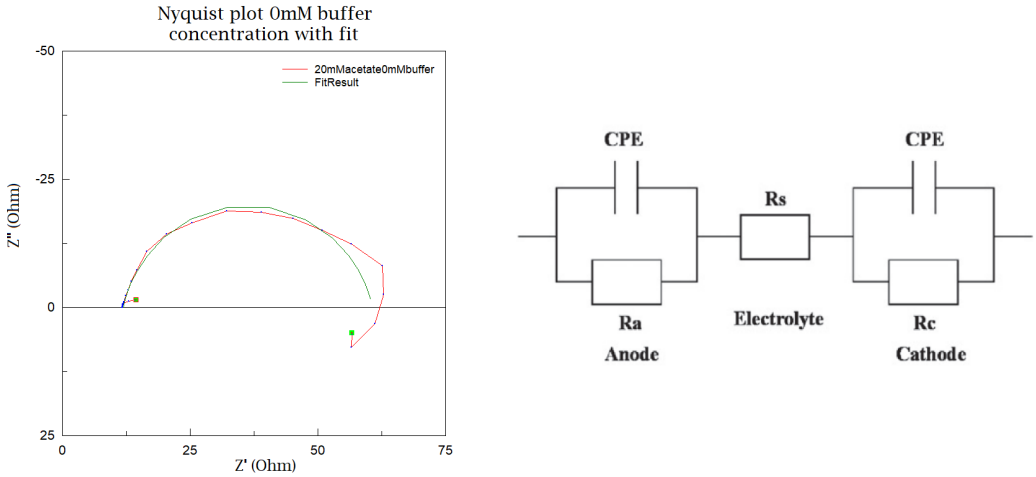

Figure 3.6: 20mM acetate 0mM buffer concentration Nyquist plot with fit (left) produced in ZView with frequency sweep from 0.398MHz to 2.512mHz. An equivalent circuit (right) is suggested by He and Mansfeld. The cathode resistance and CPE of the cathode was not used to produce the fit (anode measurement). To produce the fit the anode resistance is $48.8 \pm 1.19\Omega$, the CPE consists of CPE-T $= 0.02508 \pm 0.0009\mu$F and CPE-P $= 0.8693 \pm 0.0195$ and the electrolyte resistance is $R_s = 11.94 \pm 0.11\Omega$. [31, p. 216]

The resistances in the ECM are dominant at lower frequencies, which correspond to diffusion processes in the system. The CPEs dominate at higher frequencies, since they represent some kind of capacitors. It is possible to make similar fits for all of the different bufferconcentrations. It is also possible to plot the same fit in the Bode graphs. These Nyquist graphs however do not add value since they look very similar, which is why they are added to Appendix A. The Bode plots and their fits are also added in the attachment. The different resistances and constant phase elements are given in Table 3.1.

Table 3.1: Equivalent circuit parameters of the buffer concentration fits with constant 20mM acetate concentration

Phosphate buffer concentration	Rs (Ω)	CPE-T (μF)	CPE-P	Ra (Ω)
0 mM	11.94	0.0251	0.8693	48.8
Error	0.11	0.0009	0.0195	1.19
10 mM	8.35	0.0292	0.8321	18.83
Error	0.07	0.0015	0.0225	0.42
20 mM	6.36	0.0250	0.9017	14.08
Error	0.18	0.0045	0.0743	0.9476
50 mM	3.85	0.0347	0.8440	8.68
Error	0.06	0.0034	0.0364	0.29
100 mM	2.39	0.0680	0.8372	6.29
Error	0.04	0.0041	0.0359	0.21

Chapter 4

Discussion

The design of experiments section proposes three different setups that are possible to execute experiments. The first SMFC test matrix from Fig. 2.7 should only be used when it is not possible to create the novel designs. The low cost of this configuration is an advantage, but the sediment complicates the setup because the bacteria species are not carefully controlled. The importance of making a homogeneous sediment or solution should not be underestimated since the bacteria are the basis of the performance of every MET system. When the population mix is not distributed in the right way the power output will be influenced directly and the setup built needs to be restarted from the beginning. Controlled append of only one bacterium species in the setup over the different anode chambers will lead to a vast increase in stability and reliable results. The proposed model of Fig. 2.8 tries to stabilise these imperfections. However, it should be taken into consideration that any disturbance in the building stage could lead to a failure of the experiments later on. The time span on the experiments is at least a couple of weeks because the MFCs have to stabilise. This is another reason that the building stage has to be performed as good as possible. Although this master's thesis does not give an extensive overview in wastewater remediation of MET systems, the design in Fig. B.1 accounts the filtering effects of the microbes throughout the system. Upcoming applications and results of new research are more focused on wastewater remediation, since MFCs are the only bio-electrochemical systems that can generate electricity and break down waste [70]. Major boundaries to produce and use MFCs at large scales are the cost of the PEM, the fragile nature of the systems and the relatively small power output [71]. The latter can be investigated partly by executing the described experiments in further research.

The performance of the systems should be tested following the written protocols of current-voltage profile measurements an EIS. Multiple techniques that can be used to measure the performance of an MFC were not discussed. However, the techniques discussed can give deep insight in the internal resistances of the system, are relatively simple to execute and only need a potentiostat. It is important never to exceed the AC potential voltage delivered to the system because this can permanently harm the bacteria or destroy the system in total. It is more preferable to start with lower voltages to possible carry out the experiments multiple times than to damage the system, since it will need to be rebuilt.

The data acquired from Ter Heijne et al. is very useful to make another analysis of the buffer concentration experiments. An ECM is given in the right half of Fig. 3.6, the left part of this figure represents the anodes half cell potential. This part is approved by the fits that are made

in ZView investigating buffer concentration changes. The magnitudes of the circuit components change throughout the experiment, but the model is validated for all the different measurements. It is clear that both the solution resistances and the anode resistance decreases with increased phosphate buffer concentration. The solution conductivity is limited due to proton transport diffusion away from the anode [72]. However, increasing the buffer concentration increases the solution conductivity and therefore the solutions ability to transport more protons. The decrease in anode resistance is owing to the decrease in resistance from the charge transfer between the anode and the solution. This results in an increased activity in the bioanode and thus leads to larger current. The CPE varies without linear trend, but makes sure the high frequencies can pass from bacteria to anode. This was the reason the CPE was put into the electrical circuit, which gives another validation of the ECM. Using this analysis method is the final step in the execution of the research. When the performances of MFCs need to be tested, the different sections and steps in this master's thesis should be time consuming and easy to understand. The influence of electrode volume to surface ratio could be investigated in further research.

Chapter 5

Conclusion

A DOE test matrix has been formulated to measure the influence of electrode radius and cell volume on the electrical power output. Three models can be used: an SMFC, a cylindrical multichamber setup and a setup that also accounts for wastewater remediation. Protocols to measure the different systems are included as a roadmap to execute current-voltage profiles and EIS experiments. Fits validate the anode part of the ECM from He and Mansfeld [31]. Therefore, further characterisation of MFCs should use this ECM as a starting point when investigating the different components of MFCs. The data analysis method can be used to analyse the data and to develop ECMs for the performed experiments. The experimental investigation of electrode size could not be pursued due to the COVID-19 pandemic. However, the DOE setup, protocols and analysis methods could be a guide to continue the investigation in further research.

Bibliography

[1] M. C. Potter, "Electrical Effects Accompanying the Decomposition of Organic Compounds," *Proceedings of the Royal Society B: Biological Sciences*, vol. 84, pp. 260–276, 9 1911.

[2] B. Cohen, "The Bacterial Culture as an Electrical Half-Cell," *Journal of Bacteriology*, vol. 21, pp. 18—19, 1931.

[3] I. Karube, T. Matsunaga, S. Tsuru, and S. Suzuki, "Continous hydrogen production by immobilized whole cells of Clostridium butyricum," *BBA - General Subjects*, vol. 444, pp. 338–343, 9 1976.

[4] N. Mokhtarian, M. Ghasemi, W. R. Wan Daud, M. Ismail, G. Najafpour, and J. Alam, "Improvement of Microbial Fuel Cell Performance by Using Nafion Polyaniline Composite Membranes as a Separator," *Journal of Fuel Cell Science and Technology*, vol. 10, pp. 041008–041013, 7 2013.

[5] S. V. Mohan, S. Varjani, and A. Pandey, *Microbial electrochemical technology: Sustainable platform for fuels, chemicals and remediation*. Amsterdam: Elsevier, 1 ed., 2018.

[6] S. Venkata Mohan, R. Saravanan, S. V. Raghavulu, G. Mohanakrishna, and P. Sarma, "Bioelectricity production from wastewater treatment in dual chambered microbial fuel cell (MFC) using selectively enriched mixed microflora: Effect of catholyte," *Bioresource Technology*, vol. 99, no. 3, pp. 596–603, 2008.

[7] W. C. Lin, W. C. Lin, M. V. Coppi, M. V. Coppi, D. R. Lovley, and D. R. Lovley, "Geobacter sulfurreducens," *Society*, vol. 70, no. 4, pp. 2525–2528, 2004.

[8] D. R. Lovley, "Bug juice: Harvesting electricity with microorganisms," *Nature Reviews Microbiology*, vol. 4, no. 7, pp. 497–508, 2006.

[9] D. R. Lovley, "Microbial energizers: Fuel cells that keep on going," *Microbe*, vol. 1, no. 7, pp. 323–329, 2006.

[10] R. Nitisoravut and R. Regmi, "Plant microbial fuel cells: A promising biosystems engineering," *Renewable and Sustainable Energy Reviews*, vol. 76, no. September, pp. 81–89, 2017.

[11] A. S. Commault, G. Lear, P. Novis, and R. J. Weld, "Photosynthetic biocathode enhances the power output of a sediment-type microbial fuel cell," *New Zealand Journal of Botany*, vol. 52, no. 1, pp. 48–59, 2014.

[12] D. R. Bond and D. R. Lovley, "Electricity Production by Geobacter sulfurreducens Attached to Electrodes," vol. 69, no. 3, pp. 1548–1555, 2003.

[13] P. D. and Z. J., "Impact of electrode composition on electricity generation in a single-compartment fuel cell using Shewanella putrefaciens," *Applied Microbiology and Biotechnology*, vol. 59, pp. 58–61, 6 2002.

[14] A. K. Shukla, P. Suresh, S. Berchmans, and A. Rajendran, "Biological fuel cells and their applications," *Current Science*, vol. 87, no. 4, pp. 455–468, 2004.

[15] H. P. Bennetto, G. M. Delaney, J. R. Mason, S. D. Roller, J. L. Stirling, and C. F. Thurston, "The sucrose fuel cell: Efficient biomass conversion using a microbial catalyst," *Biotechnology Letters*, vol. 7, pp. 699–704, 10 1985.

[16] G. Reguera, K. D. McCarthy, T. Mehta, J. S. Nicoll, M. T. Tuominen, and D. R. Lovley, "Extracellular electron transfer via microbial nanowires," *Nature*, vol. 435, pp. 1098–1101, 6 2005.

[17] Y. A. Gorby, S. Yanina, J. S. McLean, K. M. Rosso, D. Moyles, A. Dohnalkova, T. J. Beveridge, I. S. Chang, B. H. Kim, K. S. Kim, D. E. Culley, S. B. Reed, M. F. Romine, D. A. Saffarini, E. A. Hill, L. Shi, D. A. Elias, D. W. Kennedy, G. Pinchuk, K. Watanabe, S. Ishii, B. Logan, K. H. Nealson, and J. K. Fredrickson, "Electrically conductive bacterial nanowires produced by Shewanella oneidensis strain MR-1 and other microorganisms.," *Proceedings of the National Academy of Sciences of the United States of America*, vol. 103, pp. 11358–63, 7 2006.

[18] R. Cornelissen, J. Manca, and V. Roland, *Centimeter-long electrical transport in cable bacteria - structural and electro-optical properties*. PhD thesis, Hasselt University, 2019.

[19] S. Pirbadian, S. E. Barchinger, K. M. Leung, H. S. Byun, Y. Jangir, R. A. Bouhenni, S. B. Reed, M. F. Romine, D. A. Saffarini, L. Shi, Y. A. Gorby, J. H. Golbeck, and M. Y. El-Naggar, "Shewanella oneidensis MR-1 nanowires are outer membrane and periplasmic extensions of the extracellular electron transport components.," *Proceedings of the National Academy of Sciences of the United States of America*, vol. 111, pp. 12883–8, 9 2014.

[20] B. E. Logan, B. Hamelers, R. Rozendal, U. Schröder, J. Keller, S. Freguia, P. Aelterman, W. Verstraete, and K. Rabaey, "Microbial fuel cells: Methodology and technology," *Environmental Science and Technology*, vol. 40, pp. 5181–5192, 9 2006.

[21] S. Jung, M. M. Mench, and J. M. Regan, "Impedance characteristics and polarization behavior of a microbial fuel cell in response to short-term changes in medium pH," *Environmental Science and Technology*, vol. 45, pp. 9069–9074, 10 2011.

[22] A. G. Capodaglio, D. Molognoni, E. Dallago, A. Liberale, R. Cella, P. Longoni, L. Pantaleoni, P. Marceta Kaninski, T. Morosuk, and P. Pei, "Microbial Fuel Cells for Direct Electrical Energy Recovery from Urban Wastewaters Academic Editors: M," *The Scientific World Journal*, vol. 2013, pp. 1–8, 2013.

[23] F. Zhao, R. C. Slade, and J. R. Varcoe, "Techniques for the study and development of microbial fuel cells: An electrochemical perspective," *Chemical Society Reviews*, vol. 38, pp. 1926–1939, 6 2009.

[24] A. K. Manohar, O. Bretschger, K. H. Nealson, and F. Mansfeld, "The use of electrochemical impedance spectroscopy (EIS) in the evaluation of the electrochemical properties of a microbial fuel cell," *Bioelectrochemistry*, vol. 72, pp. 149–154, 4 2008.

[25] G. Lepage, F. O. Albernaz, G. Perrier, and G. Merlin, "Characterization of a microbial fuel cell with reticulated carbon foam electrodes," *Bioresource Technology*, vol. 124, pp. 199–207, 2012.

[26] A. t. Heijne, D. Liu, M. Sulonen, T. Sleutels, and F. Fabregat-Santiago, "Quantification of bio-anode capacitance in bioelectrochemical systems using Electrochemical Impedance Spectroscopy," *Journal of Power Sources*, vol. 400, no. August, pp. 533–538, 2018.

[27] S. M. Tiquia-Arashiro and D. Pant, *Microbial Electrochemical Technologies*. Boca Raton: CRC Press LLC, 1 ed., 2019.

[28] C. A. Vincent and B. Scrosati, *Modern batteries : an introduction to electrochemical power sources*. Amsterdam: E. Arnold, 2 ed., 1997.

[29] N. Sekar and R. P. Ramasamy, "Electrochemical impedance spectroscopy for microbial fuel cell characterization," *Journal of Microbial and Biochemical Technology*, vol. 5, no. SPECIALISSUE.2, 2013.

[30] N. Sekar and R. P. Ramasamy, "an open access journal Biofuel Cells and Bioelectrochemical systems Citation: Sekar N, Ramasamy RP (2013) Electrochemical Impedance Spectroscopy for Microbial Fuel Cell Characterization. J Microb Biochem Technol Electrochemical Impedance Spectroscopy for Microbial Fuel Cell Characterization," *J Microbial Biochem Technol*, pp. 1948–5948, 2013.

[31] Z. He and F. Mansfeld, "Exploring the use of electrochemical impedance spectroscopy (EIS) in microbial fuel cell studies," *Energy and Environmental Science*, vol. 2, pp. 215–219, 1 2009.

[32] D. P. Strik, A. Ter Heijne, H. V. M. Hamelers, M. Saakes, and C. Buisman, "Feasibility Study on Electrochemical Impedance Spectroscopy for Microbial Fuel Cells: Measurement Modes & Data Validation," *ECS transactions*, vol. 13, pp. 27–41, 11 2008.

[33] R. Rossi and B. E. Logan, "Unraveling the contributions of internal resistance components in two-chamber microbial fuel cells using the electrode potential slope analysis," *Electrochimica Acta*, vol. 348, pp. 136291–136299, 4 2020.

[34] M. Zhou, M. Chi, J. Luo, H. He, and T. Jin, "An overview of electrode materials in microbial fuel cells," *Journal of Power Sources*, vol. 196, pp. 4427–4435, 5 2011.

[35] Y. Hindatu, M. S. Annuar, and A. M. Gumel, "Mini-review: Anode modification for improved performance of microbial fuel cell," *Renewable and Sustainable Energy Reviews*, vol. 73, pp. 236–248, 2017.

[36] H. Liu, S. Cheng, and B. E. Logan, "Power generation in fed-batch microbial fuel cells as a function of ionic strength, temperature, and reactor configuration," *Environmental Science and Technology*, vol. 39, pp. 5488–5493, 7 2005.

[37] J. Ahmed, Y. Yuan, L. Zhou, and S. Kim, "Carbon supported cobalt oxide nanoparticles-iron phthalocyanine as alternative cathode catalyst for oxygen reduction in microbial fuel cells," *Journal of Power Sources*, vol. 208, pp. 170–175, 6 2012.

[38] D. Ucar, Y. Zhang, and I. Angelidaki, "An overview of electron acceptors in microbial fuel cells," *Frontiers in Microbiology*, vol. 8, pp. 643–657, 4 2017.

[39] S. Kalathil, S. A. Patil, and D. Pant, "Microbial fuel cells: Electrode materials," in *Encyclopedia of Interfacial Chemistry: Surface Science and Electrochemistry* (Klaus Wandelt, ed.), ch. 1, pp. 309–318, Amsterdam: Elsevier, 1 2018.

[40] B. R. Dhar and H. S. Lee, "Membranes for bioelectrochemical systems: challenges and research advances," *Environmental Technology (United Kingdom)*, vol. 34, pp. 1751–1764, 7 2013.

[41] Y. L. Oon, S. A. Ong, L. N. Ho, Y. S. Wong, Y. S. Oon, H. K. Lehl, and W. E. Thung, "Hybrid system up-flow constructed wetland integrated with microbial fuel cell for simultaneous wastewater treatment and electricity generation," *Bioresource Technology*, vol. 186, pp. 270–275, 2015.

[42] P. Aelterman, K. Rabaey, H. T. Pham, N. Boon, and W. Verstraete, "Continuous Electricity Generation at High Voltages and Currents Using Stacked Microbial Fuel Cells," *Environmental Science & Technology*, vol. 40, pp. 3388–3394, 5 2006.

[43] I. Ieropoulos, J. Greenman, and C. Melhuish, "Microbial fuel cells based on carbon veil electrodes: Stack configuration and scalability," *INTERNATIONAL JOURNAL OF ENERGY RESEARCH Int. J. Energy Res*, vol. 32, pp. 1228–1240, 2008.

[44] H. Ren, H. S. Lee, and J. Chae, "Miniaturizing microbial fuel cells for potential portable power sources: Promises and challenges," *Microfluidics and Nanofluidics*, vol. 13, pp. 353–381, 9 2012.

[45] J. Winfield, I. Gajda, J. Greenman, and I. Ieropoulos, "A review into the use of ceramics in microbial fuel cells," *Bioresource Technology*, vol. 215, pp. 296–303, 9 2016.

[46] Y. Goto and N. Yoshida, "Scaling up Microbial Fuel Cells for Treating Swine Wastewater," *Water*, vol. 11, pp. 1803–1814, 8 2019.

[47] A. Janicek, Y. Fan, and H. Liu, "Design of microbial fuel cells for practical application: A review and analysis of scale-up studies," *Biofuels*, vol. 5, no. 1, pp. 79–92, 2014.

[48] S. G. Flimban, I. M. Ismail, T. Kim, and S. E. Oh, "Overview of recent advancements in the microbial fuel cell from fundamentals to applications: Design, major elements, and scalability," *Energies*, vol. 12, no. 17, pp. 3390–3410, 2019.

[49] S. Venkata Mohan, G. Mohanakrishna, G. Velvizhi, V. L. Babu, and P. N. Sarma, "Biocatalyzed electrochemical treatment of real field dairy wastewater with simultaneous power generation," *Biochemical Engineering Journal*, vol. 51, pp. 32–39, 8 2010.

[50] M. Mahdi Mardanpour, M. Nasr Esfahany, T. Behzad, and R. Sedaqatvand, "Single chamber microbial fuel cell with spiral anode for dairy wastewater treatment," *Biosensors and Bioelectronics*, vol. 38, pp. 264–269, 10 2012.

[51] Y. Feng, X. Wang, B. E. Logan, and H. Lee, "Brewery wastewater treatment using air-cathode microbial fuel cells," *Applied Microbiology and Biotechnology*, vol. 78, pp. 873–880, 4 2008.

[52] L. Zhuang, Y. Yuan, Y. Wang, and S. Zhou, "Long-term evaluation of a 10-liter serpentine-type microbial fuel cell stack treating brewery wastewater," *Bioresource Technology*, vol. 123, pp. 406–412, 11 2012.

[53] M. H. M. Nor, M. F. M. Mubarak, H. S. A. Elmi, N. Ibrahim, M. F. A. Wahab, and Z. Ibrahim, "Bioelectricity generation in microbial fuel cell using natural microflora and isolated pure culture bacteria from anaerobic palm oil mill effluent sludge," *Bioresource Technology*, vol. 190, pp. 458–465, 8 2015.

[54] G. Zhang, D. J. Lee, and F. Cheng, "Treatment of domestic sewage with anoxic/oxic membrane-less microbial fuel cell with intermittent aeration," *Bioresource Technology*, vol. 218, pp. 680–686, 10 2016.

[55] D. Jiang, M. Curtis, E. Troop, K. Scheible, J. McGrath, B. Hu, S. Suib, D. Raymond, and B. Li, "A pilot-scale study on utilizing multi-anode/cathode microbial fuel cells (MAC MFCs) to enhance the power production in wastewater treatment," *International Journal of Hydrogen Energy*, vol. 36, pp. 876–884, 1 2011.

[56] C. Jayashree, K. Tamilarasan, M. Rajkumar, P. Arulazhagan, K. N. Yogalakshmi, M. Srikanth, and J. R. Banu, "Treatment of seafood processing wastewater using upflow microbial fuel cell for power generation and identification of bacterial community in anodic biofilm," *Journal of Environmental Management*, vol. 180, pp. 351–358, 9 2016.

[57] L. Zhang, X. Yin, and S. F. Y. Li, "Bio-electrochemical degradation of paracetamol in a microbial fuel cell-Fenton system," *Chemical Engineering Journal*, vol. 276, pp. 185–192, 9 2015.

[58] Q. Wen, F. Kong, H. Zheng, D. Cao, Y. Ren, and J. Yin, "Electricity generation from synthetic penicillin wastewater in an air-cathode single chamber microbial fuel cell," *Chemical Engineering Journal*, vol. 168, pp. 572–576, 4 2011.

[59] S. R. Higgins, C. Lau, P. Atanassov, S. D. Minteer, and M. J. Cooney, "Standardized Characterization of a Flow Through Microbial Fuel Cell," *Electroanalysis*, vol. 23, pp. 2174–2181, 2011.

[60] I. Ieropoulos, J. Winfield, and J. Greenman, "Effects of flow-rate, inoculum and time on the internal resistance of microbial fuel cells," *Bioresource Technology*, vol. 101, pp. 3520–3525, 2010.

[61] L. Zhang, J. Li, X. Zhu, D. D. Ye, and Q. Liao, "Effect of proton transfer on the performance of unbuffered tubular microbial fuel cells in continuous flow mode," *International Journal of Hydrogen Energy*, vol. 40, no. 10, pp. 3953–3960, 2015.

[62] G. Sun, A. Thygesen, and A. S. Meyer, "Acetate is a superior substrate for microbial fuel cell initiation preceding bioethanol effluent utilization," *Applied Microbiology and Biotechnology*, vol. 99, pp. 4905–4915, 6 2015.

[63] Mustakeem, "Electrode materials for microbial fuel cells: Nanomaterial approach," *Materials for Renewable and Sustainable Energy*, vol. 4, no. 4, pp. 22–33, 2015.

[64] M. Ghasemi, E. Halakoo, M. Sedighi, J. Alam, and M. Sadeqzadeh, "Performance comparison of three common proton exchange membranes for sustainable bioenergy production in microbial fuel cell," *Procedia CIRP*, vol. 26, pp. 162–166, 1 2015.

[65] M. Ghasemi, W. Ramli, W. Daud, A. Fauzi Ismail, Y. Jafari, M. Ismail, A. Mayahi, and J. Othman, "Simultaneous wastewater treatment and electricity generation by microbial

fuel cell: Performance comparison and cost investigation of using Nafion 117 and SPEEK as separators," *Desalination*, vol. 325, pp. 1–6, 2013.

[66] K. J. Chae, M. Choi, F. F. Ajayi, W. Park, I. S. Chang, and I. S. Kim, "Mass Transport through a Proton Exchange Membrane (Nafion) in Microbial Fuel Cells †," *Energy and Fuels*, vol. 22, pp. 169–176, 2008.

[67] A. ter Heijne, O. Schaetzle, S. Gimenez, L. Navarro, B. Hamelers, and F. Fabregat-Santiago, "Analysis of bio-anode performance through electrochemical impedance spectroscopy," *Bioelectrochemistry*, vol. 106, pp. 64–72, 2015.

[68] M. T. Madigan, K. S. Bender, D. H. D. H. Buckley, W. M. Sattley, and D. A. Stahl, *Brock biology of microorganisms*, vol. 3. New York: Pearson, 15 ed., 1 2018.

[69] Y. Gönüllü, K. Kelm, S. Mathur, and B. Saruhan, "Equivalent circuit models for determination of the relation between the sensing behavior and properties of undoped/Cr doped TiO2 NTs," *Chemosensors*, vol. 2, no. 1, pp. 69–84, 2014.

[70] I. Gajda, J. Greenman, and I. A. Ieropoulos, "Recent advancements in real-world microbial fuel cell applications," *Current Opinion in Electrochemistry*, vol. 11, pp. 78–83, 10 2018.

[71] A. S. Mathuriya and J. V. Yakhmi, "Microbial fuel cells – Applications for generation of electrical power and beyond," *Critical Reviews in Microbiology*, vol. 42, pp. 127–143, 1 2016.

[72] C. I. Torres, A. Kato Marcus, and B. E. Rittmann, "Proton transport inside the biofilm limits electrical current generation by anode-respiring bacteria," *Biotechnology and Bioengineering*, vol. 100, pp. 872–881, 8 2008.

[73] S. Cheng, H. Liu, and B. E. Logan, "Increased power generation in a continuous flow MFC with advective flow through the porous anode and reduced electrode spacing," *Environmental Science and Technology*, vol. 40, pp. 2426–2432, 4 2006.

Appendix A

Appendix - Fits

The different Bode and Nyquist plots including fits that are discussed in Table 3.1 are given in Fig. A.1 - Fig. A.9.

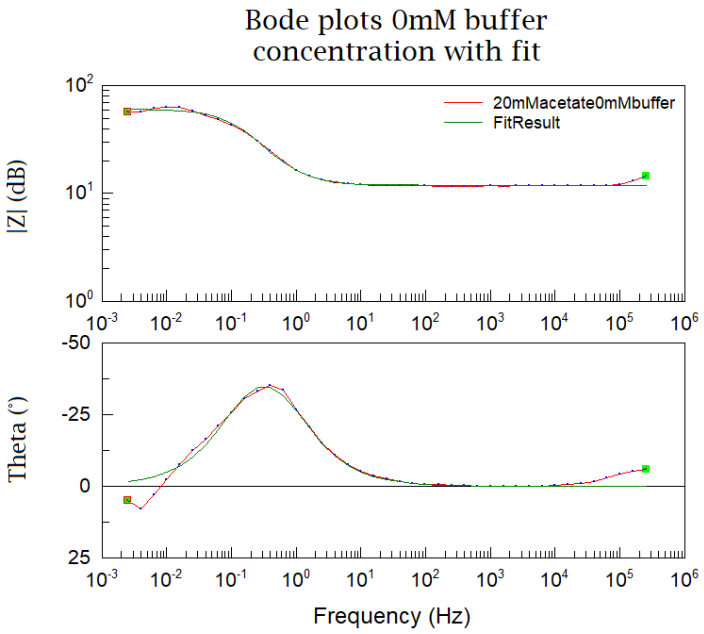

Figure A.1: 20mM acetate Bode plot with 0mM buffer concentration and fit, produced in ZView with frequency sweep from 0.398MHz to 2.512mHz

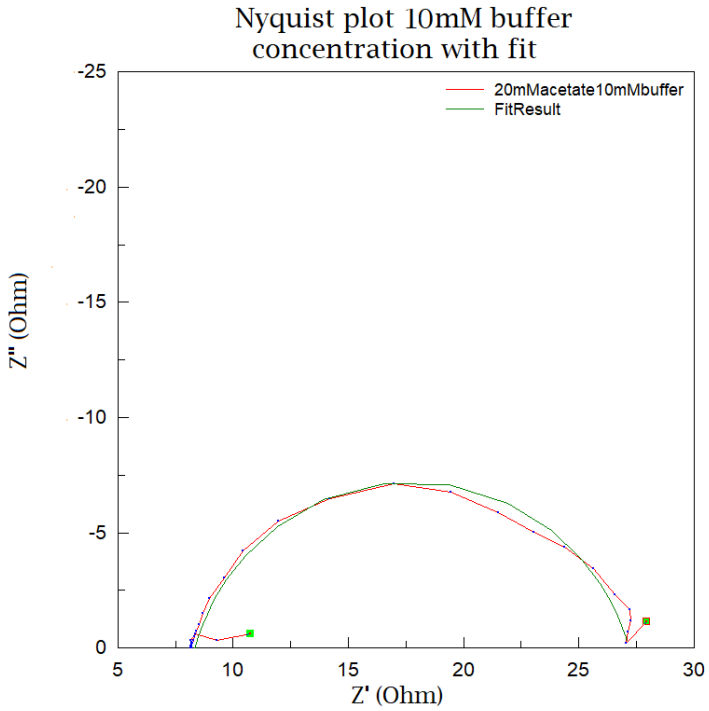

Figure A.2: 20mM acetate concentration complex plane plot with 10mM buffer concentration and fit, produced in ZView with frequency sweep from 0.398MHz to 2.512mHz

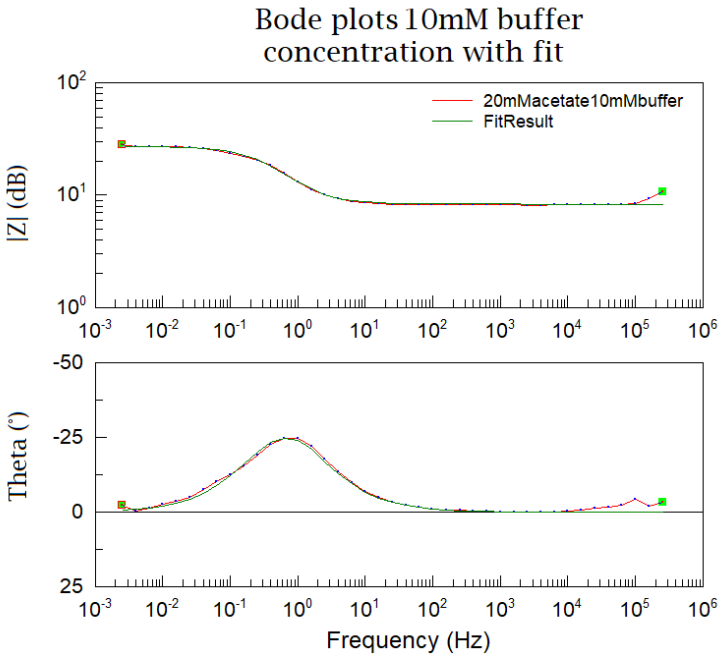

Figure A.3: 20mM acetate Bode plot with 10mM buffer concentration and fit, produced in ZView with frequency sweep from 0.398MHz to 2.512mHz

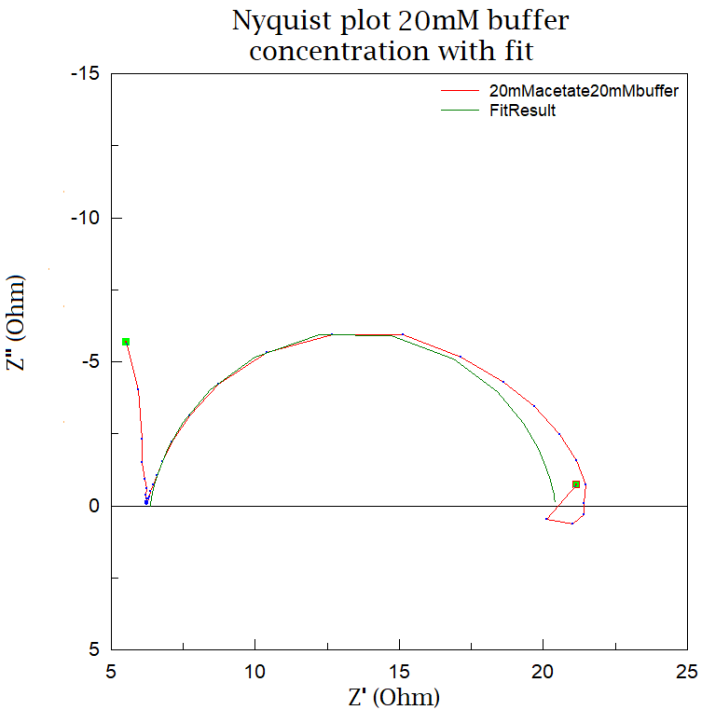

Figure A.4: 20mM acetate concentration complex plane plot with 20mM buffer concentration and fit, produced in ZView with frequency sweep from 0.398MHz to 2.512mHz

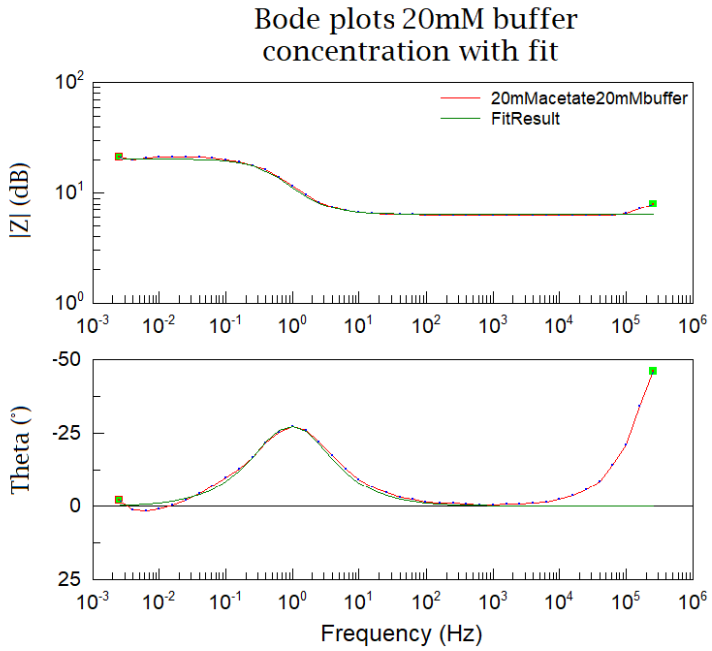

Figure A.5: 20mM acetate Bode plot with 20mM buffer concentration and fit, produced in ZView with frequency sweep from 0.398MHz to 2.512mHz

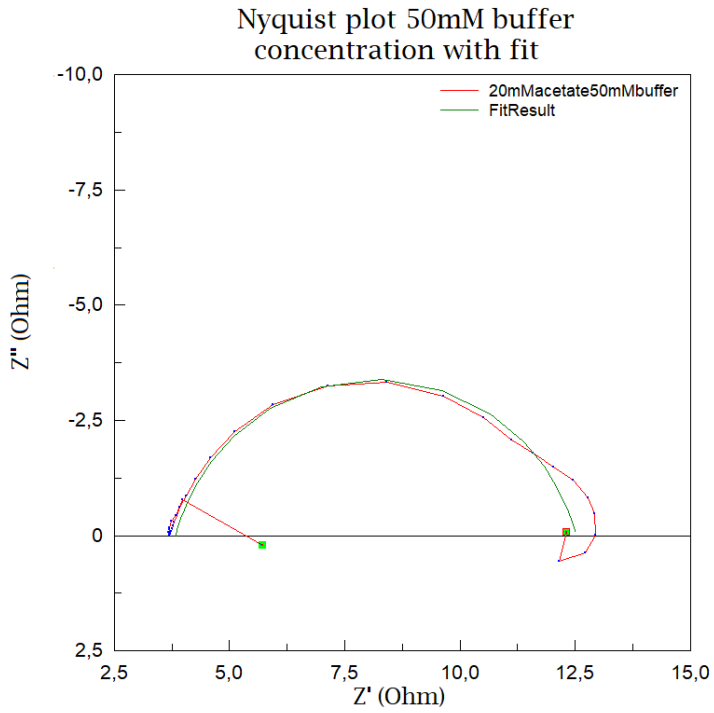

Figure A.6: 20mM acetate concentration complex plane plot with 50mM buffer concentration and fit, produced in ZView with frequency sweep from 0.398MHz to 2.512mHz

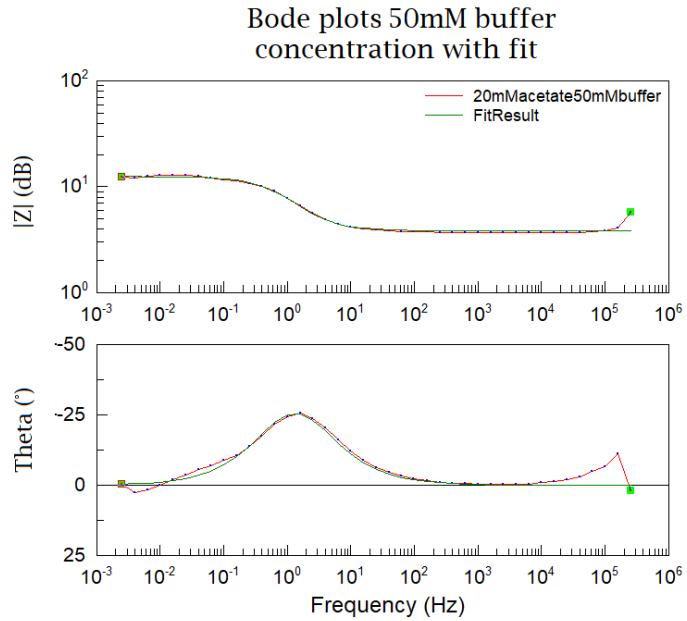

Figure A.7: 20mM acetate Bode plot with 50mM buffer concentration and fit, produced in ZView with frequency sweep from 0.398MHz to 2.512mHz

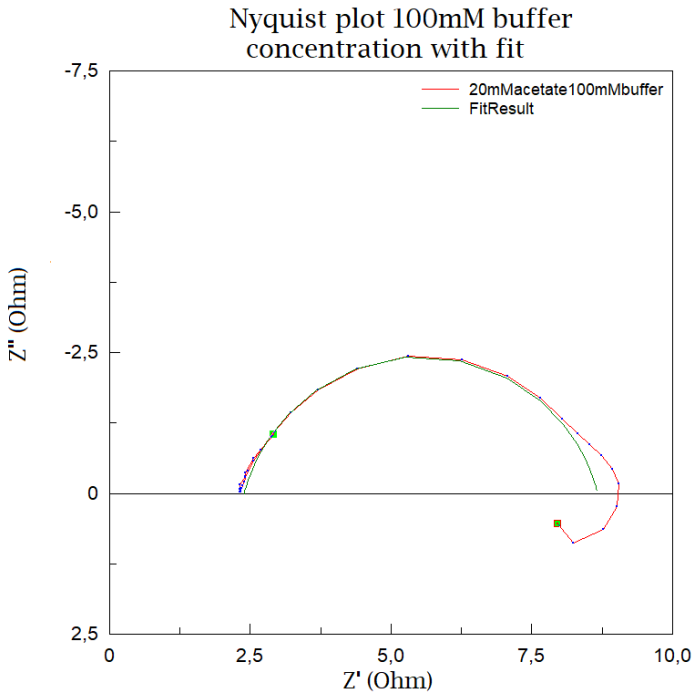

Figure A.8: 20mM acetate concentration complex plane plot with 100mM buffer concentration and fit, produced in ZView with frequency sweep from 0.398MHz to 2.512mHz

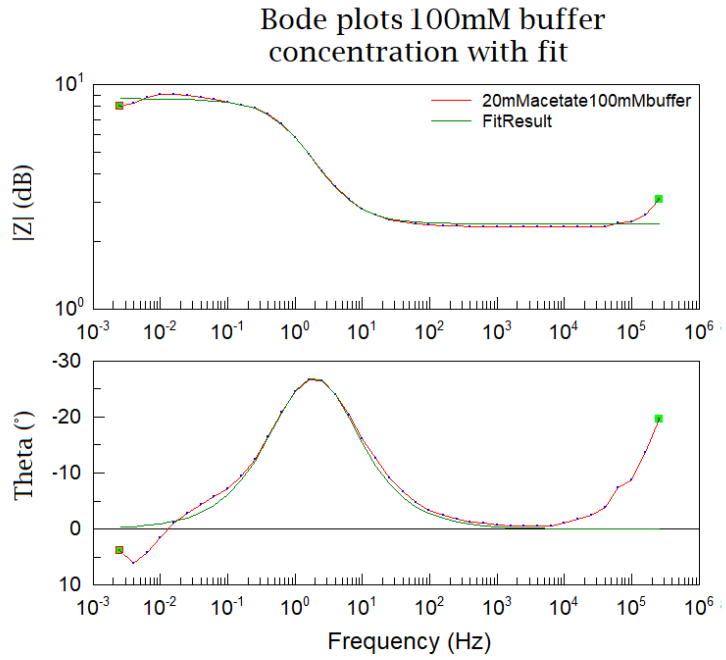

Figure A.9: 20mM acetate Bode plot with 100mM buffer concentration and fit, produced in ZView with frequency sweep from 0.398MHz to 2.512mHz

Appendix B

Appendix - Design of experiments

It is possible to measure the remediation of the aquatic substance in the anode chamber. The goal of the setup is either to investigate the electrical power output, investigate the wastewater remediation or both, all while varying volume and radius. The EIS experiments should be performed like section 2.2.3 describes.

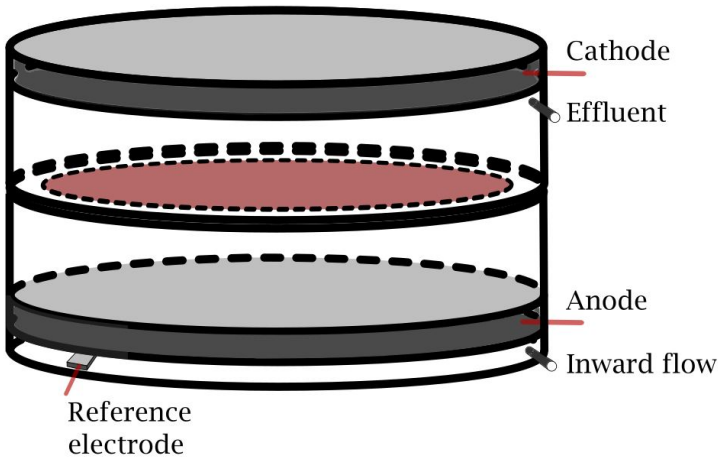

Figure B.1: Design of Experiments: the proposed lay-out for the test structure with COD removal. The graphite cathode at the top is separated from the graphite anode at the bottom by a Nafion 117 membrane (red). The inward flow at the bottom delivers new wastewater, which can be measured after remediation at the top outflow.

The difference with the test structure in Fig. 2.8 is the direction of the flow. In this setup the inward flow is at the bottom of the anode chamber, while the remediated wastewater leaves the MFC at the top in the cathode chamber. The inward flow should be controlled and measured. Typical flowrates are 1 to 50 $\frac{\text{mL}}{\text{h}}$ [60, 61, 73]. Note that if the stream is too strong between the anode and the cathode, the electrical potential reduces significantly because the electron shuttles are flushed away. The bacteria attached to the anode will filter the water by their reduction reaction. After the protons diffused through the PEM, the hydrogen is oxidised at the cathode and the filtered water can be measured at the outflow.